Polymer Dynamics and Rheology

Polymer Dynamics and Rheology

Brownian motion
Harmonic Oscillator
Damped harmonic oscillator
Elastic dumbbell model
Boltzmann superposition principle
Rubber elasticity and viscous drag
Temporary network model (Green & Tobolsky 1946)
Rouse model (1953)
Cox-Merz rule and dynamic viscoelasticity
Reptation
The gel point

The Gaussian Chain

Boltzman Probability
For a Thermally Equilibrated System

$$P_B(R) = \exp\left(-\frac{E(R)}{kT}\right)$$

Gaussian Probability
For a Chain of End to End Distance R

$$P(R) = \left(\frac{3}{2\pi\sigma^2}\right)^{3/2} \exp\left(-\frac{3(R)^2}{2(\sigma)^2}\right)$$

By Comparison The Energy to stretch a Thermally Equilibrated Chain Can be Written

$$E = kT\frac{3R^2}{2nl_K^2}$$

Force

Force

$$F = \frac{dE}{dR} = \frac{3kT}{nl_K^2}R = k_{spr}R$$

Assumptions:
-Gaussian Chain
-Thermally Equilibrated
-**Small Perturbation** of Structure (so it is still Gaussian after the deformation)

Stoke's Law

$$F = v\varsigma$$

$$\varsigma = 6\pi\eta_s R$$

Creep Experiment

$$\varepsilon_{11} = \sigma_{11}/E$$

$$d\varepsilon_{12}/dt = \sigma_{12}/\eta$$

$$\varepsilon_{11} = k\,(1 - \exp(-t/\tau))$$

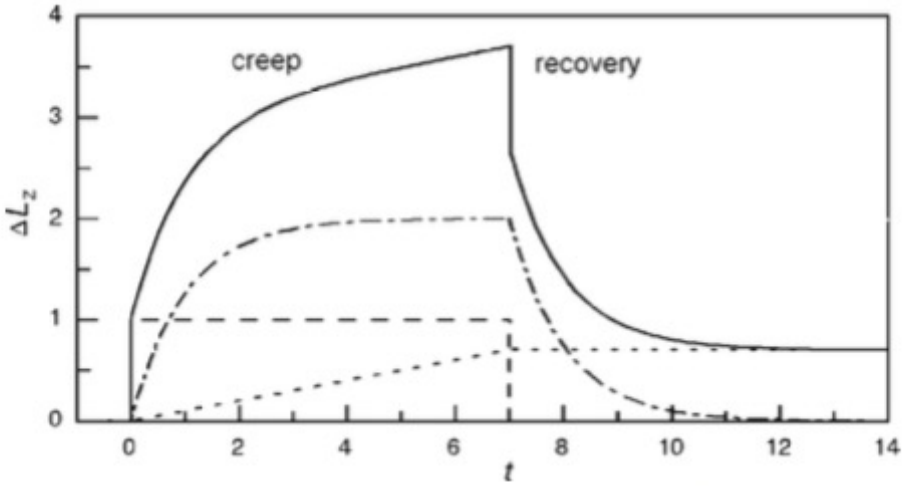

Fig. 6.1. Creep curve of a polymer sample under tension (schematic). The elongation ΔL_z induced by a constant force applied at zero time is set up by a superposition of an instantaneous elastic response (*dashed line*), a retarded anelastic part (*dash-dot line*), and viscous flow (*dotted line*). An irreversible elongation is retained after an unloading and the completion of the recovery process

$\tau = 1/\omega$ **Cox-Merz Rule**

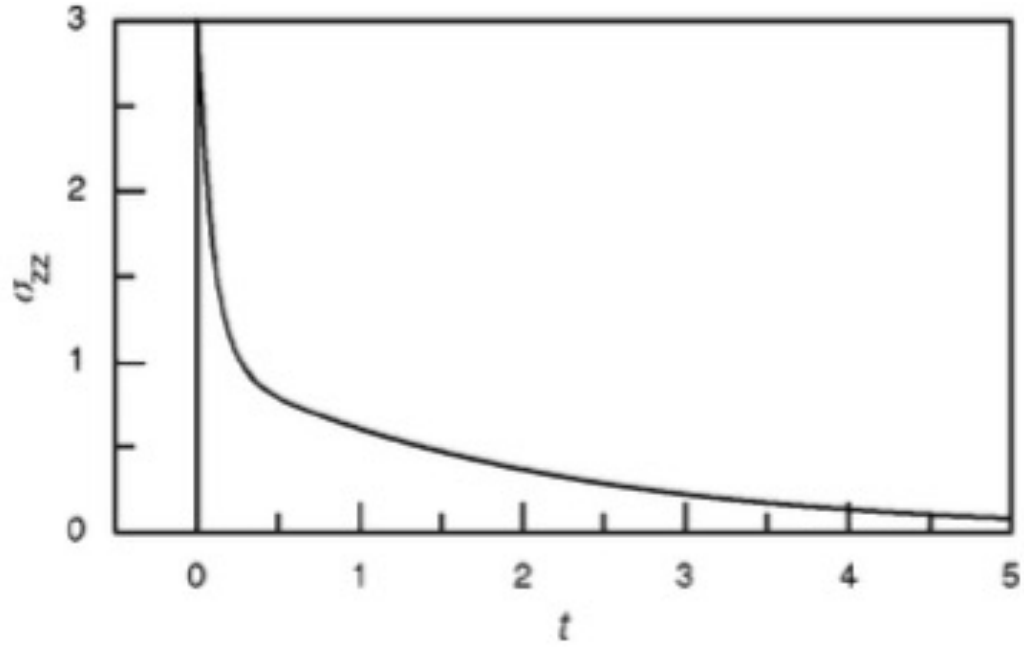

Fig. 6.2. Stress relaxation curve (schematic)

Boltzmann Superposition

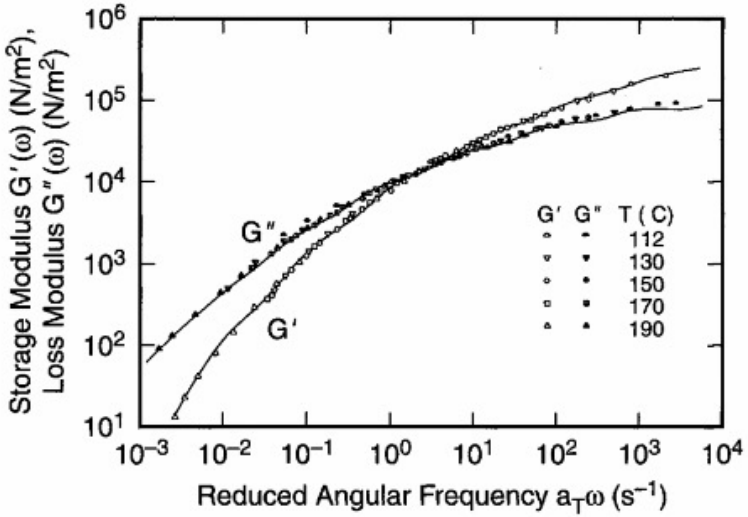

Figure 1.11 Storage and loss moduli for a low density polyethylene "Melt I." (These data were measured at several temperatures and shifted along the frequency axis by a "shift factor" a_T to form collapsed curves; see Section 3.5.2). The lines are empirical fits of Eqs. (3-25a) and (3-25b) to the data. (From Laun 1978, reprinted with permission from Steinkopff Publishers.)

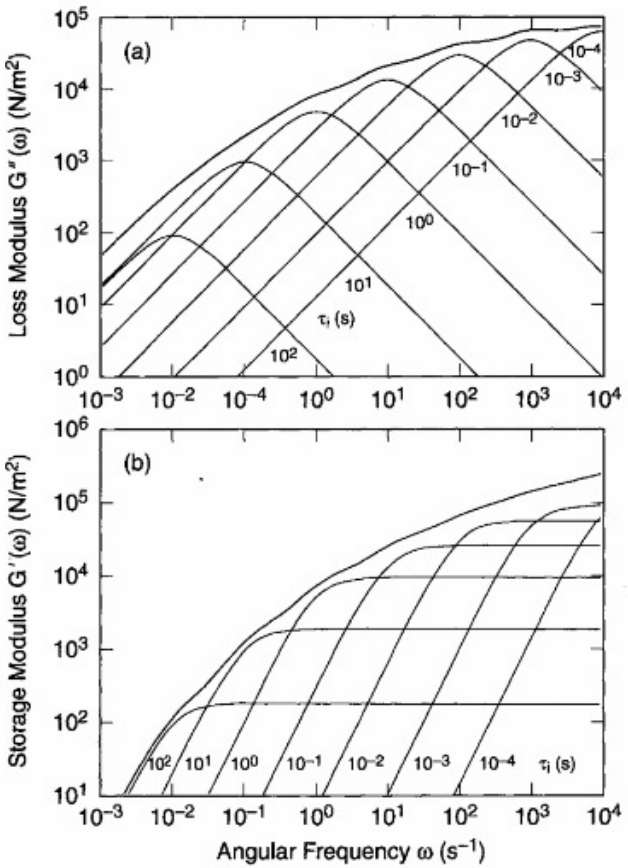

Figure 3.9 **(a)** Loss modulus G'' and **(b)** storage modulus G' versus frequency computed from Eqs. (3-25a) and (3-25b) for the eight modes given in Table 3-1 for Melt I, a polyethylene melt. Summing up over all the modes gives the "envelope" curves shown; these curves are reproduced in Fig. 1-11, where they are seen to represent accurately the linear data for this melt. (From Laun 1978, reprinted with permission from Steinkopff Publishers.)

Stress Relaxation (liquids) $E(t) = \sigma_{11}(t)/\varepsilon_{11}$

Creep (solids) $J(t) = \frac{\varepsilon(t)}{\sigma}$

Dynamic Measurement $E^*(\omega) = \sigma_{11}(t)/\varepsilon_{11}(t)$

$$\sigma_{11}(t) = \sigma^0_{11} \exp(i\omega t)$$

$$\varepsilon_{11}(t) = \varepsilon^0_{11} \exp(-i\delta) \exp(i\omega t)$$

Harmonic Oscillator: $\delta = 90^\circ$ for all ω except $\omega = 1/\tau$ where $\delta = 0^\circ$

Hookean Elastic $\delta = 0°$

Newtonian Fluid $\delta = 90°$

$$e^{-iA} = \cos A - i \sin A \qquad e^{+iA} = \cos A + i \sin A$$

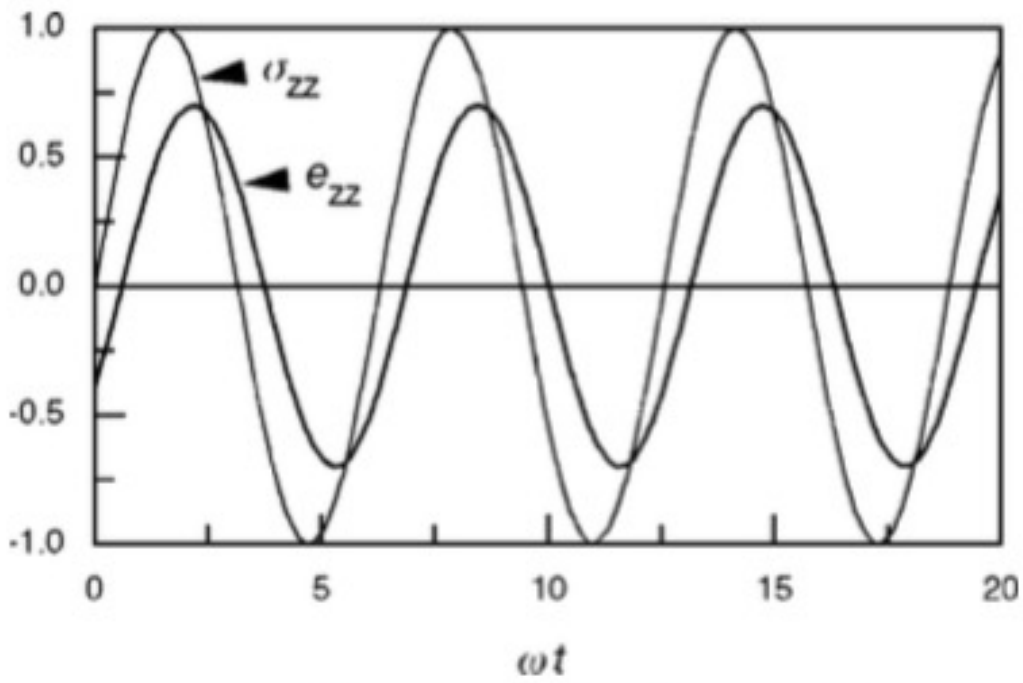

Fig. 6.3. Time dependence of stress (σ_{zz}) and strain (e_{zz}) in a dynamic-mechanical experiment (schematic)

Brownian Motion

$$\langle V(t) \rangle = 0$$

$$\langle V(t_1)V(t_2) \rangle = C_v(t_1 - t_2)$$

$C_v(t)$ is the velocity correlation function

correlation time, τ_V

$$\langle V(t_1)V(t_2) \rangle = \langle V(t)V(0) \rangle = C_v(t)$$

$\langle V^2(t) \rangle = kT/m$ For short times $E = kT = \frac{1}{2} mV^2$

For long times $\langle V^2(t) \rangle = 0$

$$m\,(dV/dt) = -6\pi\eta_s a\, V \qquad F = ma = \zeta V$$

$$V = V_0 \exp(-6\pi\eta_s a\,(t_1 - t_2)/m) = V_0 \exp(-(t_1 - t_2)/\tau_V)$$ Integrate

$$\tau_V = m/(6\pi\eta_s a)$$

For a sphere of density ρ, $m = (4\pi/3)a^3$, and $\tau_V = (2\pi/9)\rho\, a^2/\eta_s$.

The relaxation time, τ_V, is very small for colloidal scale objects such as polymer coils, $O(10^{-10}s)$

polymer in dilute solution $\tau_V \approx 0$

displacement $\xi(t) = \int_0^t V(t')dt'$

$$\langle \xi(t)^2 \rangle = \int_0^t dt_1 \int_0^t \langle V(t_1)V(t_2)\rangle dt_2 = 2Dt = \int_0^t dt_1 \int_0^t 2D\delta(t_1 - t_2)dt_2$$

$$<V(t_1)V(t_2)> = <V(t)V(0)> = 2D\delta(t)$$

Brownian Motion in a Potential Field:

$$\langle V \rangle = -(1/\zeta)dU/dx = \langle dx/dt \rangle,$$

$$dE = F\,dx$$
$$F = \zeta V$$

$$dx/dt = -(1/\zeta)dU/dx + g(t)$$ **Langevin Equation**

$$\langle g(t) \rangle = 0$$

$$\langle g(t)g(t') \rangle = 2D\delta(t-t')$$

$$\langle V(t_1)V(t_2) \rangle = \langle V(t)V(0) \rangle = 2D\delta(t)$$

Brownian Motion of a Harmonic Oscillator:

$$U(x) = kx^2/2$$

$F = kdx$

$Fdx = dU$

Langevin Equation

$$dx/dt = -kx/\zeta + g(t)$$

$dx/dt = -(1/\zeta)dU/dx + g(t)$

http://mathworld.wolfram.com/First-OrderOrdinaryDifferentialEquation.html

$$x(t) = \int_{-\infty}^{t} dt' \, e^{-k(t-t')/\zeta} g(t')$$

$$\langle x(t)x(0)\rangle = \int_{-\infty}^{t} dt_1 \int_{-\infty}^{0} dt_2 \exp\left[-k(t-t_1-t_2)/\zeta\right]\langle g(t_1)g(t_2)\rangle$$

Using $\langle g(t)g(t')\rangle = 2D\delta(t-t')$ and $D = kT/\zeta$,

$$\langle x(t)x(0)\rangle = kT\exp(-t/\tau)/k_{spr}$$

$$\tau = \zeta/k_{spr}$$

For $t \Rightarrow 0$, $\langle x^2\rangle = kT/k_{spr}$, as predicted by a Boltzman distribution, $\Psi_{equil} \alpha \exp(-k_{spr}x^2/2kT)$

$$\left\langle (x(t)-x(0))^2 \right\rangle = \left\langle x(t)^2 \right\rangle + \left\langle x(0)^2 \right\rangle - 2\langle x(t)x(0)\rangle$$

$$= 2\left\langle x^2 \right\rangle - 2\langle x(t)x(0)\rangle$$

$$= 2kT/k_{spr}\left(1-\exp(-t/\tau)\right)$$

For t=>0 this yields $(2kT/\zeta)t = 2Dt$ which is the expected result from the discussion of Brownian motion above.

General Linear Response Theory:

$\psi(t)$ as the kind of force that is applied when you strike a bell

$$x(t) = \psi_0 \, \mu(t)$$

the primary response function

$\mu(t)$

describes the response of a material to an infinitely short, pulsed force or field, $\psi(t) = \psi_0 \, \delta(t)$

$\delta(t)$, has a value of ∞ for a given t
The integral with respect to time is 1.

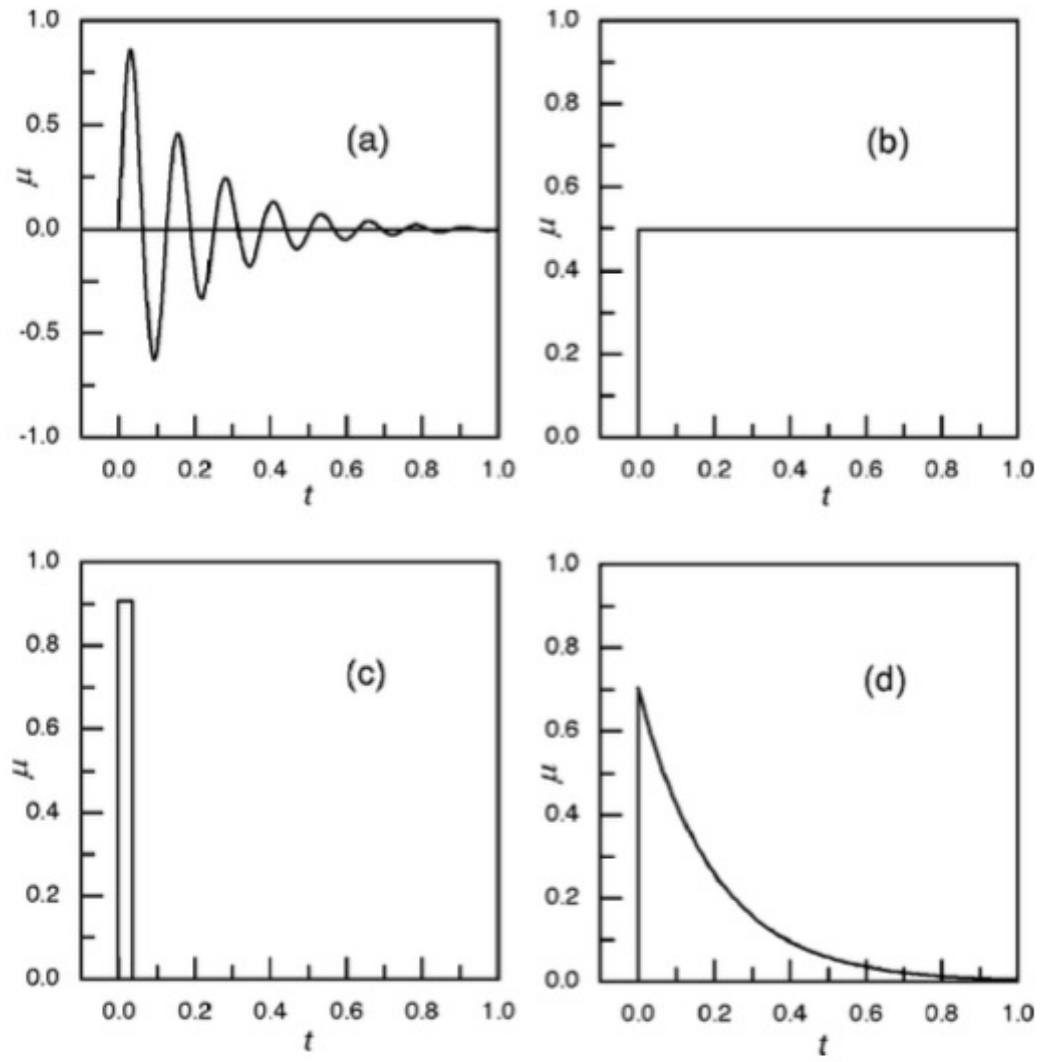

Fig. 6.4. Primary response function of a damped harmonic oscillator (**a**), a perfectly viscous body (**b**), a Hookean solid (**c**), and a simple relaxatory system (**d**)

The response to any force field

$$x(t) = \int_{-\infty}^{t} \mu(t - t')\psi(t')dt'$$

The latter expression relies on two assumptions:

1) Causality principle, the response is caused by the field or force that the material experienced in the past;

2) Superposition principle, the field or force over time can be described by a sequence of pulses and the response is a summation of the responses to these pulses.

Relationships Between Different Dynamic Measurements:

Creep Measurement:

Following Strobl, p. 200, consider a creep experiment where a stress, $\psi(t)$, is applied to a sample at t=0, for t>0; $\psi(t) = \psi_0$. The creep, x(t), is given by

$$x(t) = \int_0^t \mu(t - t')\psi_0 \, dt'$$

For this constant stress experiment the displacement, x(t) can be directly normalized by the force, ψ_0, to yield the susceptibility, $\alpha(t)$, or the integral of the response function, or the cumulative response function.

$$\frac{x(t)}{\psi_0} = \int_0^t \mu(t - t')dt' = \int_0^t \mu(t'')dt''$$

we can also write that the response function is the derivative of the **time dependent susceptibility**,

$$\mu(t) = \frac{d\alpha}{dt}(t)$$

Stress Relaxation Measurment:

In the stress relaxation experiment the strain is fixed, $x(t) = x_0$, while the stress relaxes, $\psi(t)$,

$$x_0 = \int_0^t \mu(t-t')\psi(t')dt'$$

It is natural to reduce the stress, $\psi(t)$, by the fixed strain, x_0, to yield a **time dependent modulus**, $a(t) = \psi(t)/x_0$. Then,

$$1 = \int_0^t \mu(t-t')a(t')dt' = \int_0^t \frac{d\alpha}{dt}(t-t')a(t')dt'$$

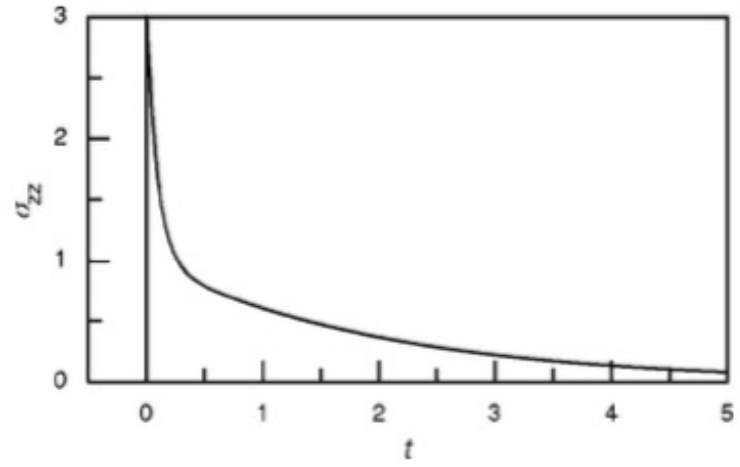

Fig. 6.2. Stress relaxation curve (schematic)

Boltzman Superposition Equation:

If the susceptibility is used in the definition of the response function we have,

$$x(t) = \int_{-\infty}^{t} \mu(t-t')\psi(t')dt' = \int_{-\infty}^{t} \frac{d\alpha}{dt}(t-t')\psi(t')dt'$$

The latter expression can be reduced using integration by parts;

$$\int udv = uv - \int vdu$$

where u = ψ(t') and dv = (da/dt') dt', so v = a(t') and du = dψ(t'), then,

$$x(t) = \int_{-\infty}^{t} \alpha(t-t')d\psi(t')$$

The latter expression indicates that the integral over all time till now of the change in force times the susceptibility yields the response. This equation indicates that the load on a sample can be broken down into differential steps and the response can be obtained by integration of these steps times the susceptibility of the material to loading.

A similar analysis can be made using the definition of the time dependent modulus, a(t), to describe the corollary of the Boltzman equation for creep,

$$\psi(t) = \int_{-\infty}^{t} a(t-t')dx(t')$$

The force at time t, ψ(t), is composed of incremental steps of strain, dx, times the time dependent modulus, a(t).

Dynamic Mechanical Measurements:

In a dynamic mechanical measurement an oscillating force, $\psi(t) = \psi_0 \exp i\omega t = \psi_0 (\cos \omega t + i \sin \omega t)$, is applied to the sample and the strain response displays a time lag (phase angle difference), δ, so the strain is written, $x(t) = x_0 \exp -i\delta \exp i\omega t = x_0 \exp i(\omega t - \delta)$. Using,

$$x(t) = \int_0^t \mu(t-t')\psi(t')dt'$$

and substituting the dynamic expressions,

$$x_0 \exp\{i(\omega t - \delta)\} = \int_{-\infty}^{t} \mu(t-t')\psi_0 \exp\{i\omega t'\}dt'$$

The dynamic susceptibility, $\alpha^*(\omega)$, can be obtained in analogy to the creep experiment, $\alpha^*(\omega) = \{x_0 \exp -i\delta\}/\psi_0$. The dynamic susceptibility is related to the primary response function, $\mu(t)$, by,

$$\alpha^*(\omega) = \int_{-\infty}^{t} \mu(t-t')\exp\{i\omega(t-t')\}dt' = \int_0^{\infty} \mu(t'')\exp\{-i\omega t''\}dt'' = \int_{-\infty}^{\infty} \mu(t'')\exp\{-i\omega t''\}dt''$$

the latter equality being due to $\mu = 0$ below t=0. Then the complex susceptibility is the Fourier transform of the primary response function, $\mu(t)$!

Kramers-Kronig Dispersion Relations:

The dynamic susceptibility is a complex function, $\alpha^*(\omega) = \alpha'(\omega) - i\,\alpha''(\omega)$. The imaginary part, $\alpha''(\omega)$, reflects the loss (Hookean response for susceptibility); while the real part, $\alpha'(\omega)$, reflects motion of the material (flow). Each of these parts are related to the primary response function, $\mu(t)$, that is a real function. This can be easily demonstrated by expansion of the complex exponential,

$$\alpha'(\omega) - i\alpha''(\omega) = \left\{\int_{-\infty}^{\infty} \mu(t)\cos(\omega t)dt\right\} - i\left\{\int_{-\infty}^{\infty} \mu(t)\sin(\omega t)dt\right\}$$

Both loss and storage are based on the primary response function, so it should be possible to express a relationship between the two.

The response function is not defined at $t = \infty$ **or at** $\omega = 0$
This leads to a singularity where you can't do the integrals

Cauchy Integral

$$P\left(\int_{-\infty}^{\infty} \frac{\alpha''}{\omega - \omega_0} d\omega\right) = \lim_{\phi \to 0}\left[\int_{-\infty}^{\omega_0 - \phi} \frac{\alpha''}{\omega - \omega_0} d\omega + \int_{\omega_0 + \phi}^{\infty} \frac{\alpha''}{\omega - \omega_0} d\omega\right]$$

$$P\left(\int_{-\infty}^{\infty}\frac{\alpha''}{\omega-\omega_0}d\omega\right)=\lim_{\phi\to 0}\left[\int_{-\infty}^{\omega_0-\phi}\frac{\alpha''}{\omega-\omega_0}d\omega+\int_{\omega_0+\phi}^{\infty}\frac{\alpha''}{\omega-\omega_0}d\omega\right]$$

Then the Kramers-Kronig dispersion relations can be written using the Cauchy integral as,

$$\alpha'(\omega)=\frac{1}{\pi}P\left[\int_{-\infty}^{\infty}\frac{\alpha''(\omega)}{\omega-\omega_0}d\omega\right]$$

$$\alpha''(\omega)=\frac{1}{\pi}P\left[\int_{-\infty}^{\infty}\frac{\alpha'(\omega)}{\omega-\omega_0}d\omega\right]$$

Power Consumption (Rate of Work) in a Dynamic Measurement:

The power consumption, (dW/dt)/V, in a perturbation, ψ(t), response, x(t) observation is given by,

W energy = Force * distance

$$\frac{1}{V}\frac{dW}{dt} = \psi \frac{dx}{dt}$$

$$\psi(t) = \psi_0 \cos \omega t$$

$$dx(t)/dt = -\omega\alpha' \psi_0 \sin \omega t + \omega\alpha'' \psi_0 \cos \omega t$$

$$\frac{1}{V}\frac{dW}{dt} = \psi \frac{dx}{dt} = \omega\varphi_0^2 \cos(\omega t)\{\alpha'' \cos(\omega t) - \alpha' \sin(\omega t)\} = \omega\varphi_0^2 \left\{ \alpha'' \cos^2(\omega t) - \frac{\alpha'}{2} \sin(2\omega t) \right\}$$

heat generated — energy of oscillation 0 over time

$$\sin(x)\cos(x) = \sin(2x)/2$$

Dynamic Dielectric Measurements:

$$\underline{D} = \varepsilon_0 \underline{E} + \underline{P} = \varepsilon_0 \varepsilon \underline{E}$$ Dielectric Displacement

Parallel Analytic Technique to Dynamic Mechanical
(Most of the math was originally worked out for dielectric relaxation)

Simple types of relaxation can be considered, water molecules for instance.

$\mathbf{P} = \varepsilon_0(\varepsilon - 1)\,\mathbf{E}$, $\mathbf{D} = \varepsilon_0 \varepsilon\,\mathbf{E}$ dielectric displacement

P is the resulting polarization

E is an applied electric field

ε_0 Free Space

ε Material

ε_u Dynamic material

Creep: a constant field $\mathbf{E}_0$

$$\mathbf{P}(t) = \varepsilon_0(\varepsilon_u - 1)\,\mathbf{E}_0 + \varepsilon_0\,\Delta\varepsilon(t)\,\mathbf{E}_0$$

Instantaneous Response — Time-lag Response

Dynamic:

$\mathbf{E}(t) = \mathbf{E}_0 \exp i\omega t$, $\mathbf{P}(t) = \exp i(\omega t - \delta)$

$$\varepsilon^*(\omega) = \varepsilon'(\omega) - i\,\varepsilon''(\omega) = \varepsilon_0 + P_0\,(\exp -i\delta)/E_0$$

Modes of Relaxation

water molecules.

$$\mathbf{P}_{or} \approx \{\rho\, p^2\, E/(3kT)\}$$ Rotational Motion at Equilibrium

p is the dipole moment of the water molecules

electric field, **E**.

A single relaxation mode, τ relaxation

100/e % or 36.8% of the molecules have reached the equilibrium state

Single-Time Relaxation Processes:

Creep Measurement

σ_{12}^{0} is applied at time t = 0 and the strain $\gamma_{12}(t)$ develops with time

Response

$\Delta J\ \sigma_{12}^{0}$, where ΔJ is called the *relaxation strength*

$d\gamma_{12}(t)/dt$, changes with time and reaches 0 when the system is at equilibrium

$$\gamma_{12}(t) = \Delta J\ \sigma_{12}^{0}$$

a *linear decay*

$dx/dt = -kx/\zeta + g(t)$

$$d\gamma_{12}(t)/dt = K\ (\gamma_{12}(t) - \Delta J\ \sigma_{12}^{0}) \qquad K = 1/\tau$$

$$\gamma_{12}(t) = \Delta J \sigma_{12}^{0}(1 - \exp(-t/\tau))$$

http://mathworld.wolfram.com/First-OrderOrdinaryDifferentialEquation.html

limiting conditions of $\gamma = 0$ at
t=0 or for the t=∞ limit of $\gamma = \Delta J\ \sigma_{12}^{0}$

Apply to a dynamic mechanical measurement

$$d\gamma_{12}(t)/dt = K\,(\gamma_{12}(t) - \Delta J\,\sigma_{12}^{0})$$

$$\gamma_{12}(t) = \Delta J \sigma_{12}^{0}\left(1 - \exp(-t/\tau)\right)$$

$$\Delta J\,\sigma_{12}^{0}; \qquad \Delta J\,\sigma_{12}(t) \qquad \sigma_{12}(t) = \sigma_{12}^{0}\exp(i\omega t)$$

$$d\gamma_{12}(t)/dt = (-1/\tau)\,(\gamma_{12}(t) - \Delta J\,\sigma_{12}^{0}\exp(i\omega t))$$

$$\gamma_{12}(t) = \sigma_{12}^{0}\,J^{*}(\omega)\exp(i\omega t)$$

$$\frac{d\gamma_{12}(t)}{dt} = i\omega\sigma_{12}^{0}J^{*}(\omega)\exp(i\omega t)$$

$$J^{*}(\omega) = \frac{\Delta J}{1 + i\omega\tau}$$

Single mode
Debye Relaxation

Multiply by $\frac{(i\omega\tau - 1)}{(i\omega\tau - 1)}$

$$J^{*}(\omega) = J' - iJ'' = \frac{\Delta J}{1+\omega^{2}\tau^{2}} - i\frac{\Delta J\omega\tau}{1+\omega^{2}\tau^{2}}$$

Single mode
Debye Relaxation

$$J^*(\omega) = J' - iJ'' = \frac{\Delta J}{1+\omega^2\tau^2} - i\frac{\Delta J\omega\tau}{1+\omega^2\tau^2}$$

$$\Delta J\omega\tau/(1+\omega^2\tau^2) = \Delta J/\{(1/\omega\tau)+\omega\tau\} = \Delta J/\{10^{-\log\omega\tau}+10^{\log\omega\tau}\}$$

Symmetric on a log-log plot

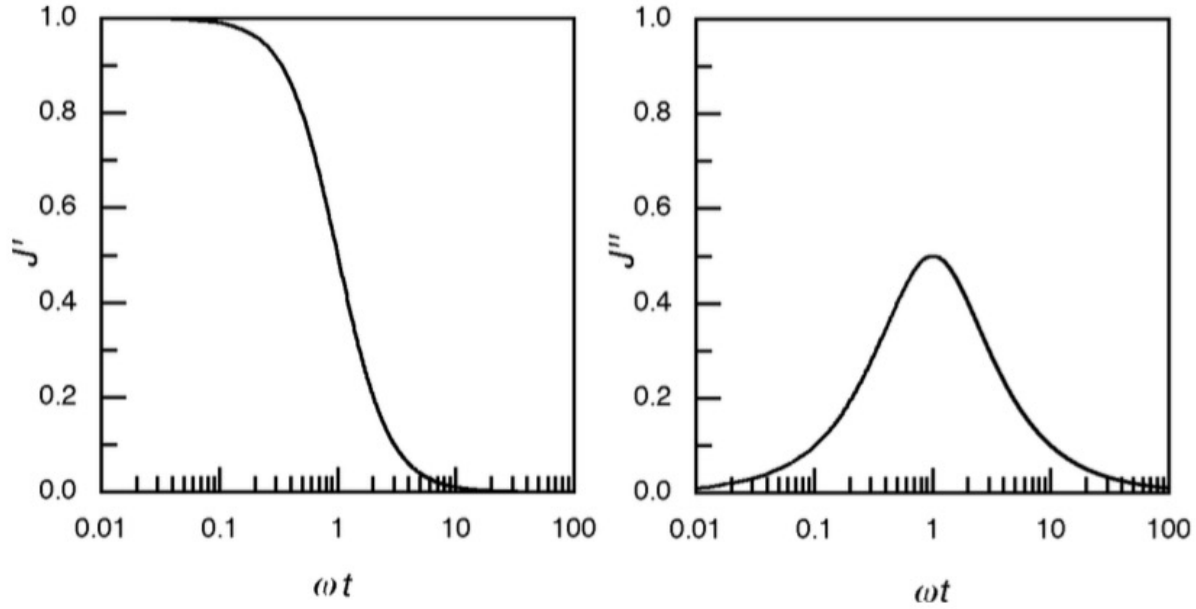

Fig. 6.5. Real part (*left*) and imaginary part (*right*) of the dynamic compliance associated with a mechanical Debye process

Relationship between the Loss and Storage Compliance for a Debye-Process:

$$J^*(\omega) = J' - iJ'' = \frac{\Delta J}{1+\omega^2\tau^2} - i\frac{\Delta J\omega\tau}{1+\omega^2\tau^2}$$

$$\Delta J\omega\tau/(1+\omega^2\tau^2) = \Delta J/\{(1/\omega\tau)+\omega\tau\} = \Delta J/\{10^{-\log\omega\tau}+10^{\log\omega\tau}\}$$

$$\int_{-\infty}^{\infty} J''\,\mathrm{d}\log(\omega\tau) = \frac{\pi}{2\ln 10}\Delta J$$

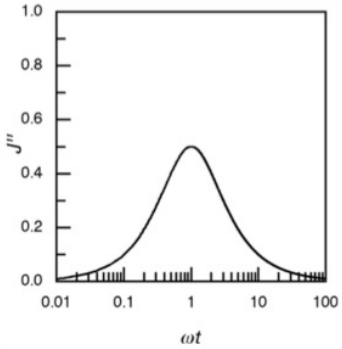

Kramers-Kronig dispersion relations

$$\alpha'(\omega) = \frac{1}{\pi}P\left[\int_{-\infty}^{\infty}\frac{\alpha''(\omega)}{\omega-\omega_0}d\omega\right]$$

$$\alpha''(\omega) = \frac{1}{\pi}P\left[\int_{-\infty}^{\infty}\frac{\alpha'(\omega)}{\omega-\omega_0}d\omega\right]$$

"impossible to have a loss
compliance without a corresponding
(in frequency) change in the storage compliance"

Single mode
Debye Relaxation

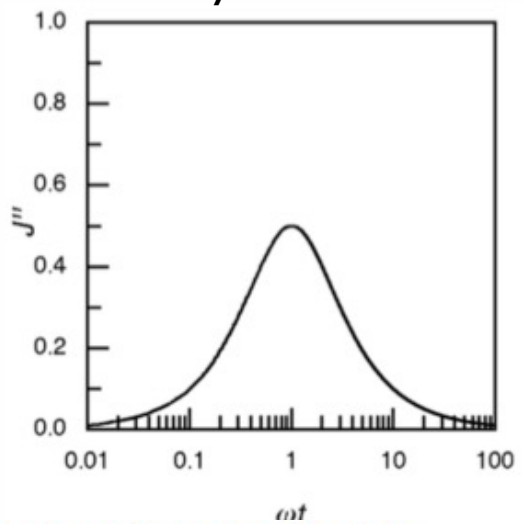

The total width at half-height is 1.2 decades.
lower limit for a relaxation process

More complex processes have a broader peak

harmonic oscillator is single valued

a damped harmonic oscillator

Shows a broader peak but much narrower than a Debye relaxation

The width of the loss peak indicates the difference
between a vibration and a relaxation process

Oscillating system displays a moment of inertia
Relaxing system only dissipates energy

Cole-Cole Plot:

Equation for a circle in J'-J'' space

$$(x-x_0)^2 + (y-y_0)^2 = K^2$$

$$J^*(\omega) = J' - iJ'' = \frac{\Delta J}{1+\omega^2\tau^2} - i\frac{\Delta J\omega\tau}{1+\omega^2\tau^2}$$

$$\left(J' - \frac{\Delta J}{2}\right)^2 + J''^2 = \left\{\frac{\frac{\Delta J}{2}\left(1-\omega^2\tau^2\right)}{1+\omega^2\tau^2}\right\}^2 + \left\{\frac{\frac{\Delta J}{2}2\omega\tau}{1+\omega^2\tau^2}\right\}^2 = \frac{\Delta J^2}{4}\left\{\frac{1+2\omega^2\tau^2+\omega^4\tau^4}{\left(1+\omega^2\tau^2\right)^2}\right\}$$

$$= \frac{\Delta J^2}{4}\left\{\frac{\left(1+\omega^2\tau^2\right)^2}{\left(1+\omega^2\tau^2\right)^2}\right\} = \frac{\Delta J^2}{4}$$

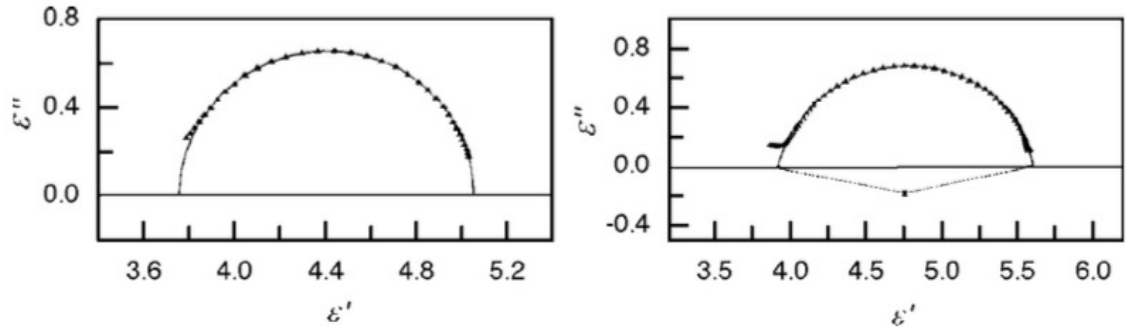

Fig. 6.6. Cole–Cole plots of dielectric data obtained for a dipole carrying a rod-like molecule of low molar mass (*left*) and a polysiloxane with these molecules attached as side-groups (*right*) [67]

Cole-Cole Plot:

$$\left[\varepsilon' - \left(\varepsilon_u + \frac{\Delta\varepsilon}{2}\right)\right]^2 + (\varepsilon'')^2 = \frac{\Delta\varepsilon^2}{4}$$

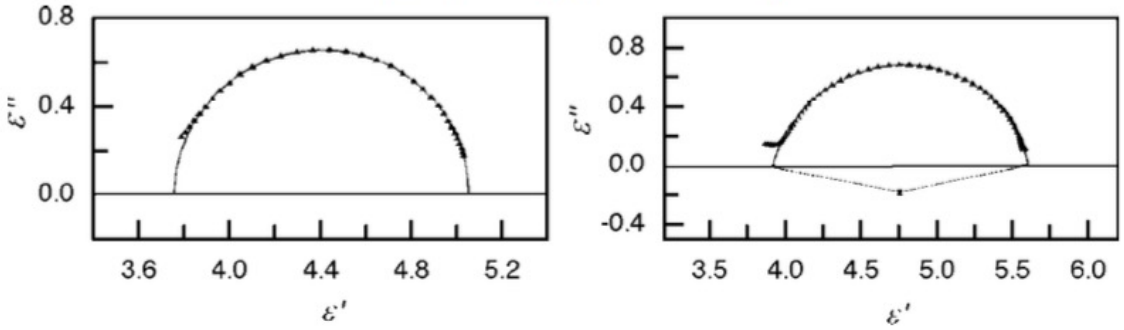

Fig. 6.6. Cole–Cole plots of dielectric data obtained for a dipole carrying a rod-like molecule of low molar mass (*left*) and a polysiloxane with these molecules attached as side-groups (*right*) [67]

The left curve is for a rod molecule with a strong dipole moment that displays a simple Debye-process relaxation. The instantaneous polarization, ε_u, is about $\varepsilon_u = 3.73$ which is determined at the left of the plot ($\omega \Rightarrow \infty$ limit). The right intercept, $\varepsilon' = \varepsilon_u + \Delta\varepsilon$, is at about 5.06 so $\Delta\varepsilon = 1.33$. The peak occurs at about $\varepsilon'' = \Delta\varepsilon/2 = 0.67$ for $\varepsilon' = \varepsilon_u + \Delta\varepsilon/2 = 4.40$.

The right curve is for the same rod-like chemical group attached as a side-group to a polymer chain. For the Debye-process (left curve) we had $\varepsilon^*(\omega\tau) = \varepsilon_u + \Delta\varepsilon/(1 + i\,\omega\tau) = \varepsilon_u + \Delta\varepsilon\,(1 - \omega\tau) / \{(1 - \omega\tau)\,(1 + i\,\omega\tau)\} = \varepsilon_u + \Delta\varepsilon/(1 + \omega^2\tau^2) - i\omega\tau\,\Delta\varepsilon/(1 + \omega^2\tau^2)$. A comparison between the simple single-valued relaxation time, Debye-process of the left curve and the deviatory process of the right curve include:

1) Shift of ε_u from 3.73 to about 3.89 (larger instantaneous polarization)
2) Shift of $\Delta\varepsilon$ from 1.33 to 1.71 (larger relaxation strength, $\Delta\varepsilon$)
3) The center of the relaxation circle occurs at $\varepsilon' = 4.75$ which remains close to $\varepsilon' = \varepsilon_u + \Delta\varepsilon/2$.
4) Peak value is lower than $\varepsilon'' = \Delta\varepsilon/2$, $\varepsilon''_{peak} = 0.69$ (compare to the expected value of 0.86).

Deviations from the Debye-process in the right curve can be modeled by a Cole-Cole Function that includes a scaling parameter, β, $\varepsilon^*(\omega\tau) = \varepsilon_u + \Delta\varepsilon/(1 + i\,\omega\tau)^{1-\beta}$, where $\beta = 0$ for a Debye-process. Expansion of this equation yields a coupling between the imaginary and real relaxation terms, $\varepsilon^*(\omega\tau) = \varepsilon_u + \Delta\varepsilon(1 - i\omega\tau)^{1-\beta}/(1 + \omega^2\tau^2)^{1-\beta}$.

Time Dependent Value

Equilibrium Value

$$\frac{d\gamma}{dt} = -\frac{\gamma(t)}{\tau} + \Delta J \sigma_0$$

Relaxation Spectra:

$J^*(\omega)$ ΔJ $\sigma_{12}(t)$ $\sigma_{12}(t) = \sigma_{12}^{\ 0} \exp(i\omega t)$

$d\gamma_{12}(t)/dt = (-1/\tau)\ (\gamma_{12}(t) - \Delta J \sigma_{12}^{\ 0} \exp(i\omega t))$

$\gamma_{12}(t) = \sigma_{12}^{\ 0}\, J^*(\omega) \exp(i\omega t)$

By substitution of this expression into the differential equation and solving for the dynamic compliance, $J^*(\omega)$,

$$J^*(\omega) = \frac{\Delta J}{1 + i\omega\tau}$$

$$J^*(\omega) = J' - iJ'' = \frac{\Delta J}{1+\omega^2\tau^2} - i\frac{\Delta J\omega\tau}{1+\omega^2\tau^2}$$

A linear sum of Debye-processes is the simplest description of a series of relaxation processes each with a strength of relaxation, ΔJ_l and a time constant τ_l,

$$J^*(\omega) = J_u + \sum_l \frac{\Delta J_l}{1 + i\omega\tau_l}$$

Lodge Liquid
Boltzmann Superposition

$$J^*(\omega) = J_u + \int \frac{L_J(\log\tau)}{1 + i\omega\tau} d(\log\tau)$$

$L_J(\log \tau)$ is called the retardation time spectrum.

For a creep measurement, the strain with time is given by $\gamma_{12}(t) = \Delta J \sigma^{0}_{12} (1\text{-}\exp(-t/\tau))$. The retardation time spectrum, $L_J(\log\tau)$ can be used to describe the creep of a complex material with a relaxation spectrum,

$$J(t) = J_u \Theta(t) + \int \left\{1 - \exp\frac{-t}{\tau}\right\} L_J(\log\tau) d(\log\tau)$$

where $\Theta(t)$ is 1 for $t>0$ and 0 for $t<0$.

$$J^*(\omega) = J_u + \Delta J/(1 + i\omega\tau))$$

$$G^*(\omega) = 1/J^*(\omega)$$

substituting $J_r = J_u + \Delta J$ $\underline{\tau} = \tau\, J_u/J_r$, $G_u = 1/J_u$, $G_r = 1/J_r$, and $\Delta G = G_u - G_r$

$$G^*(\omega) = G_u + \Delta G/(1+ i\omega\underline{\tau})$$

$$G^*(\omega) = G_u - \int \frac{H_G(\log\hat{\tau})}{1+i\omega\hat{\tau}} d(\log\hat{\tau})$$

$$G(t) = G_u\Theta(t) + \int \left\{\exp\frac{-t}{\hat{\tau}}\right\} H_G(\log\hat{\tau}) d(\log\hat{\tau})$$

$H_G(\log\underline{\tau})$ is called the relaxation time spectrum for the material.

Boltzmann Superposition

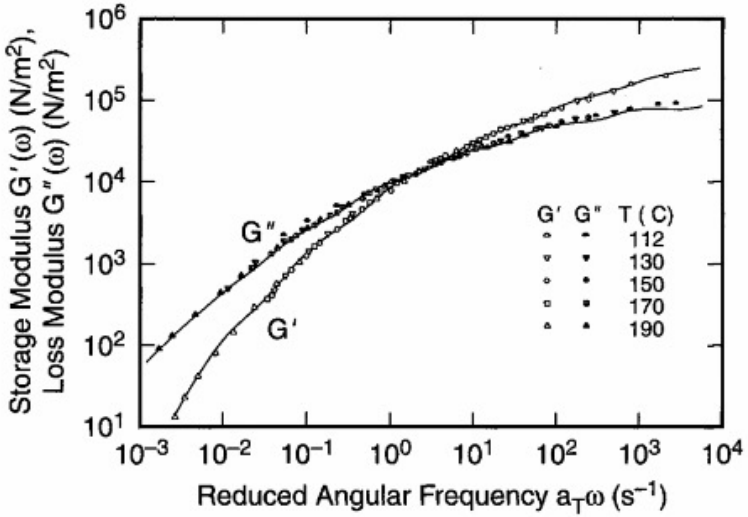

Figure 1.11 Storage and loss moduli for a low density polyethylene "Melt I." (These data were measured at several temperatures and shifted along the frequency axis by a "shift factor" a_T to form collapsed curves; see Section 3.5.2). The lines are empirical fits of Eqs. (3-25a) and (3-25b) to the data. (From Laun 1978, reprinted with permission from Steinkopff Publishers.)

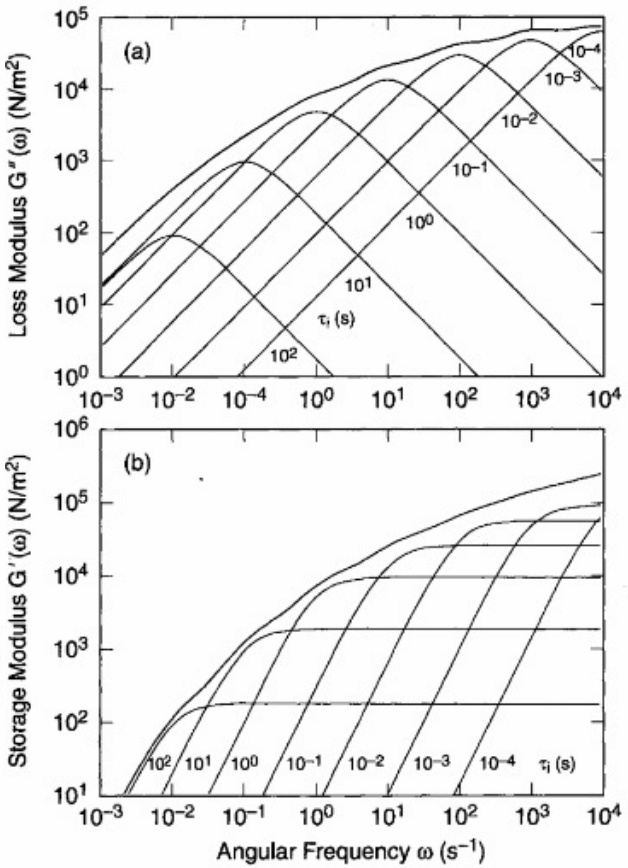

Figure 3.9 **(a)** Loss modulus G'' and **(b)** storage modulus G' versus frequency computed from Eqs. (3-25a) and (3-25b) for the eight modes given in Table 3-1 for Melt I, a polyethylene melt. Summing up over all the modes gives the "envelope" curves shown; these curves are reproduced in Fig. 1-11, where they are seen to represent accurately the linear data for this melt. (From Laun 1978, reprinted with permission from Steinkopff Publishers.)

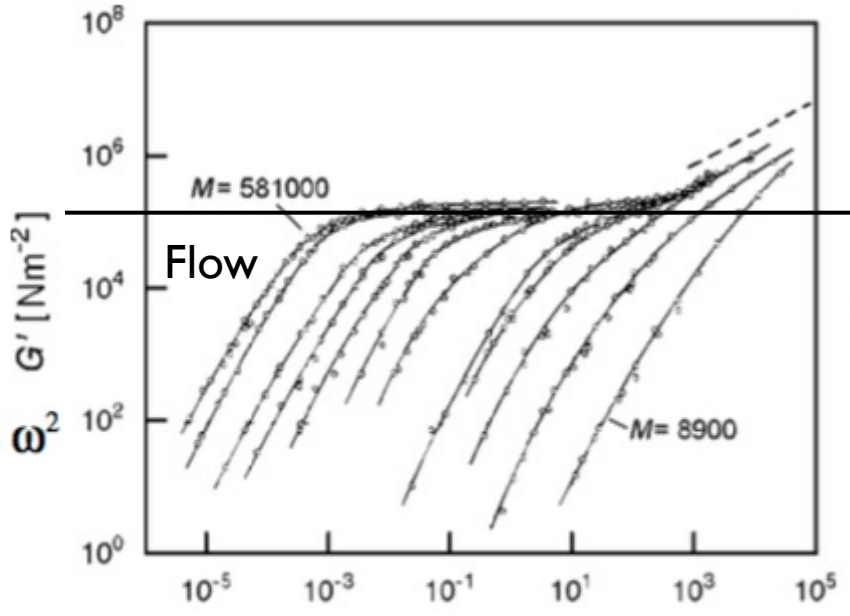

Flow

Rouse Dynamics

$$G'(\omega) \propto (\eta_0 \omega)^{1/2}$$

G'(ω), follows ω^2

Newtonian fluid there would be no storage shear modulus, G'

Fig. 6.16. Storage shear moduli measured for a series of fractions of PS with different molar masses in the range $M = 8.9 \times 10^3$ to 5.81×10^5 g mol^{-1}. The *dashed line in the upper right corner* indicates the slope corresponding to the power law Eq. (8.82) derived for the Rouse model of the glass transition. Data from Onogi et al. [74]

Following the plateau regime a second power law regime is observed in the log-log plot of figure 5.15. The slope in this regime is 2 for a frequency plot and –2 for a time plot, $G'(\omega) = K'_\eta \omega^2$ or $E(t) = K_\eta t^{-2}$.

$$dJ'/dt = d\gamma_{12}(t)/dt\ (1/\sigma_{12}) = 1/\eta$$

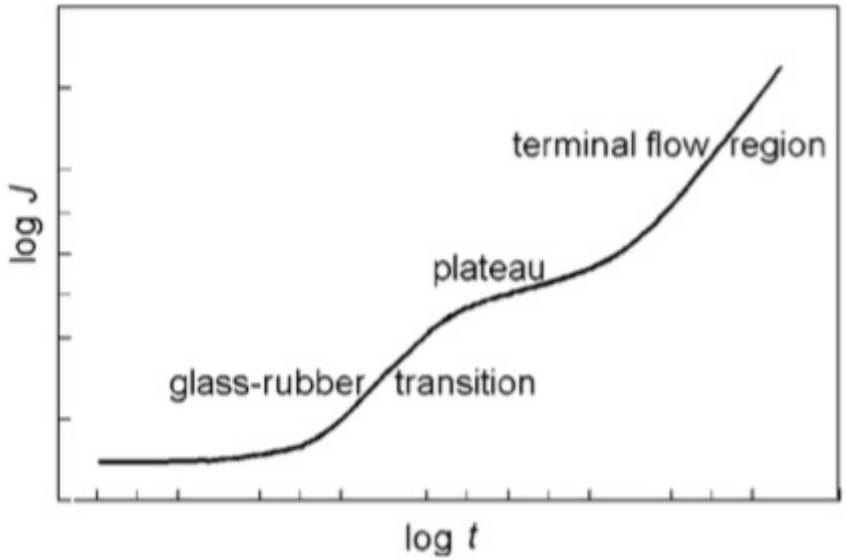

Fig. 6.12. General shape of the complete creep curve of PS, as suggested by the appearance of the different parts shown in Fig. 6.11

For a Newtonian fluid, $\sigma_{xy} = \eta_0 \, d\gamma_{xy}/dt$. If a Newtonian fluid is measured in a dynamic compliance experiment, where, $\sigma_{xy} = \sigma_{xy}^{\,0} \exp(i\omega t)$ and $\gamma = J^*\sigma_{xy}^{\,0} \exp(i\omega t)$. Taking the derivative of the strain and inserting into Newton's law of viscosity yields,

$$J^* = -i/(\eta_0\omega)$$

The Newtonian fluid differs from a polymeric melt in that the Newtonian fluid does not display a recoverable shear compliance, $J_e^{\,0}$, associated with elasticity of the melt. At the zero-shear rate limit the dynamic compliance for a polymeric fluid is given by,

$$J^*(\omega=>0) = J_e^{\,0} - i/(\eta_0\omega)$$

Then, the recoverable shear compliance is the real part of the zero shear rate compliance, J', and the zero-shear rate viscosity is related to the imaginary part of the zero shear rate compliance, J".

By taking the inverse of J* we can obtain G* as.

$$G^*(\omega=>0) = J_e^0 (\omega\eta_0)^2 + i (\omega\eta_0)$$

Then we have well defined power-laws in frequency for G* and J* at the zero shear rate limit (low frequency regime) and the recoverable shear compliance and zero shear rate viscosity are the primary parameters of importance. The ω^2 dependence is shown in the first plot of this chapter (G' versus ω in figure 5.15).

Newtonian Flow

Entanglement Reptation

Rouse Behavior

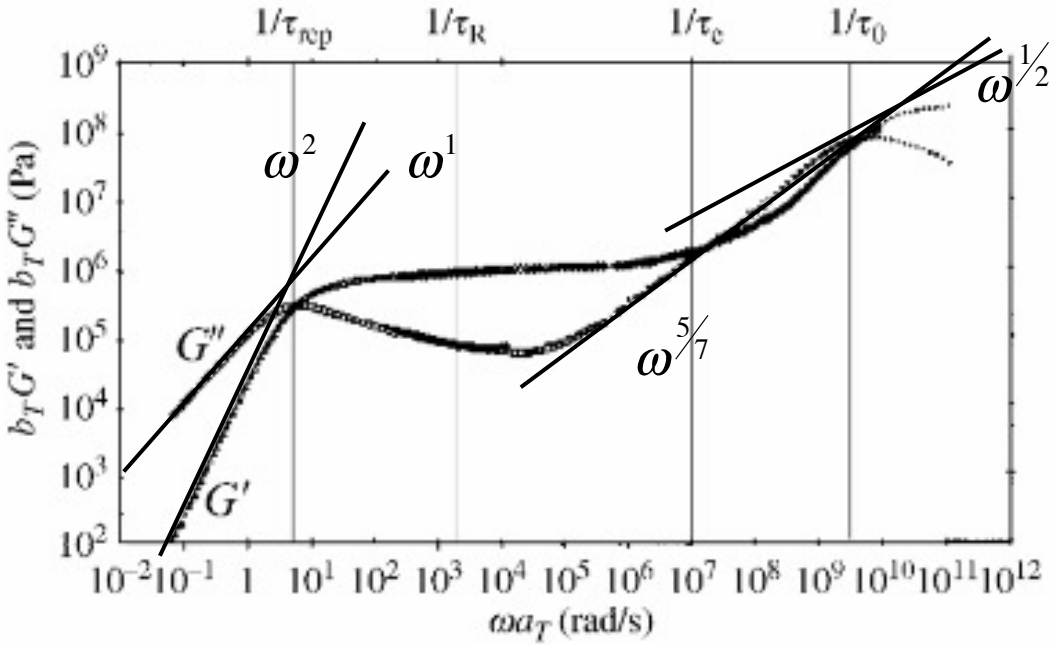

Fig. 9.3
Master curve at 25 °C from oscillatory shear data at six temperatures for a 1,4-polybutadiene sample with $M_w = 130\,000\ \mathrm{g\,mol^{-1}}$. Data from R. H. Colby, L. J. Fetters and W. W. Graessley, *Macromolecules* **20**, 2226 (1987).

$$\psi(t) = \int_{-\infty}^{t} a(t-t')dx(t')$$

and the viscosity, η, is the stress, $\psi(t)$, divided by the strain rate, de/dt, so the zero shear rate viscosity, η_0, (at infinite time, $t = \infty$) in a shear experiment where there is no strain before time t=0, is given by,

$$\eta_0 = \int_{0}^{\infty} G(t)dt$$

The time dependent modulus, a(t) or here G(t), is related to the primary response function by:

$$\mu(t) = dG(t)/dt$$

J_e^0 can also be related to the time dependent modulus and the primary response function by considering a dynamic mechanical experiment where $e(t) = e_0 \exp(i\omega t)$ and $\sigma(t) = G^* e(t)$. Using the above equation for the Boltzman superposition principle:

$$\sigma(t) = \int_{-\infty}^{t} G(t-t')\dot{e}(t')dt'$$

taking the derivative of the strain, $de/dt = i\omega \exp(i\omega t)$ and substituting $t'' = t-t'$,

$$G^* = \int_{t''=0}^{\infty} G(t'')i\omega e^{-i\omega t''}dt''$$

For $\omega \Rightarrow 0$, the exponential can be expanded, $\exp(-iA) = 1 + A + \ldots$, so,

$$G'(\omega \Rightarrow 0) = \omega^2 \int_{t=0}^{\infty} tG(t)dt$$

$$G''(\omega \Rightarrow 0) = \omega \int_{t=0}^{\infty} G(t)dt$$

The first expression can be coupled with the previous expression for G', $G' = J_e^0 (\omega\eta_0)^2$, to yield a description of J_e^0,

$$J_e^0 \eta_0^2 = \int_0^{\infty} tG(t)dt$$

The ratios of the two integrals that define J_e^0 and η_0, yields a time,

$$\bar{\tau} = \frac{\int_0^\infty tG(t)dt}{\int_0^\infty G(t)dt} = J_e^0\eta_0$$

This time is called the mean viscoelastic relaxation time. For non-entangled melts (below M_e) this time is proportional to the molecular weight squared. For entangled melts it is proportional to the moleculare weight to the 3.4 power. This is because for entangled melts J_e^0 is constant (plateau) and the time is proportional to the viscosity that increases with a 3.4 power experimentally. Below the entanglement molecular weight both J_e^0 and the zero shear rate viscosity are proportional to M (as will be discussed later).

$$\eta(\dot{\gamma}) = \sigma_{zx}/\dot{\gamma}$$

$$\Psi_1(\dot{\gamma}) = (\sigma_{xx} - \sigma_{zz})/(\dot{\gamma})^2$$

$$\Psi_2(\dot{\gamma}) = (\sigma_{yy} - \sigma_{zz})/(\dot{\gamma})^2$$

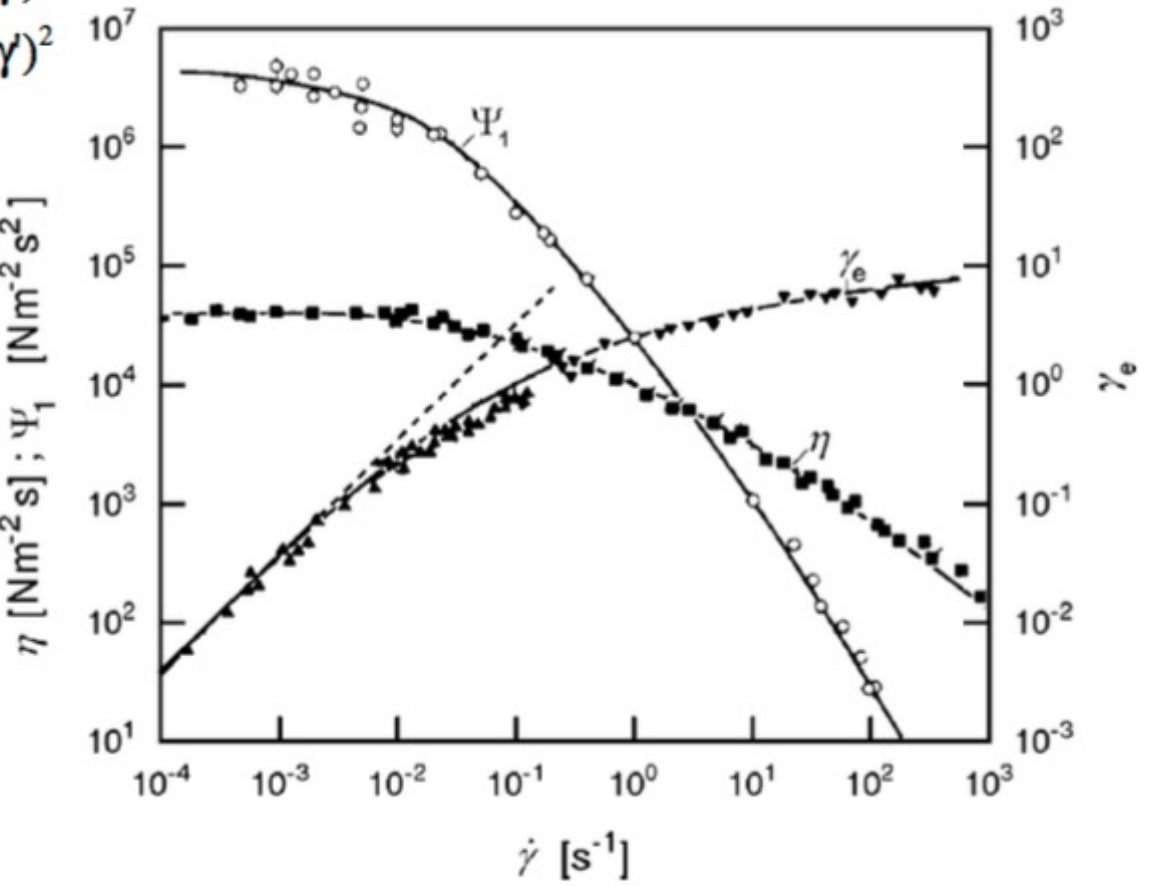

Fig. 9.17. PE under steady state shear flow at 150 °C: Strain rate dependencies of the viscosity η, the primary normal stress coefficient Ψ_1 and the recoverable shear strain γ_e. The *dotted line* represents Eq. (9.157). Results obtained by Laun [116]

Figure 7.15 shows the recoverable shear strain, γ_e, that is proportional to the recoverable shear compliance, $J_e = \gamma_e/\sigma_{zx}$. At low strain rates the recoverable shear strain is just linear in the rate of strain as indicated by the dashed line. The linear behavior occurs in the regime where the viscosity and first normal stress coefficient are constant. In fact, the dashed line follows a linear function of the viscosity and first normal stress coefficient,

$$\gamma_e(\dot{\gamma}=>0) = (\Psi_1(\dot{\gamma}=>0) / \{2\,\eta(\dot{\gamma}=>0)\})\,\dot{\gamma} = (\sigma_{xx} - \sigma_{zz})/(2\,\sigma_{zx})$$

then,

$$J_e^{\,0} = \gamma_e(\dot{\gamma}=>0)/\sigma_{zx} = \Psi_{1,0}/(2\,\eta_0^{\,2})$$

At low shear rates there remain only two independent parameters that describe polymeric flow.

Newtonian Flow

Entanglement Reptation

Rouse Behavior

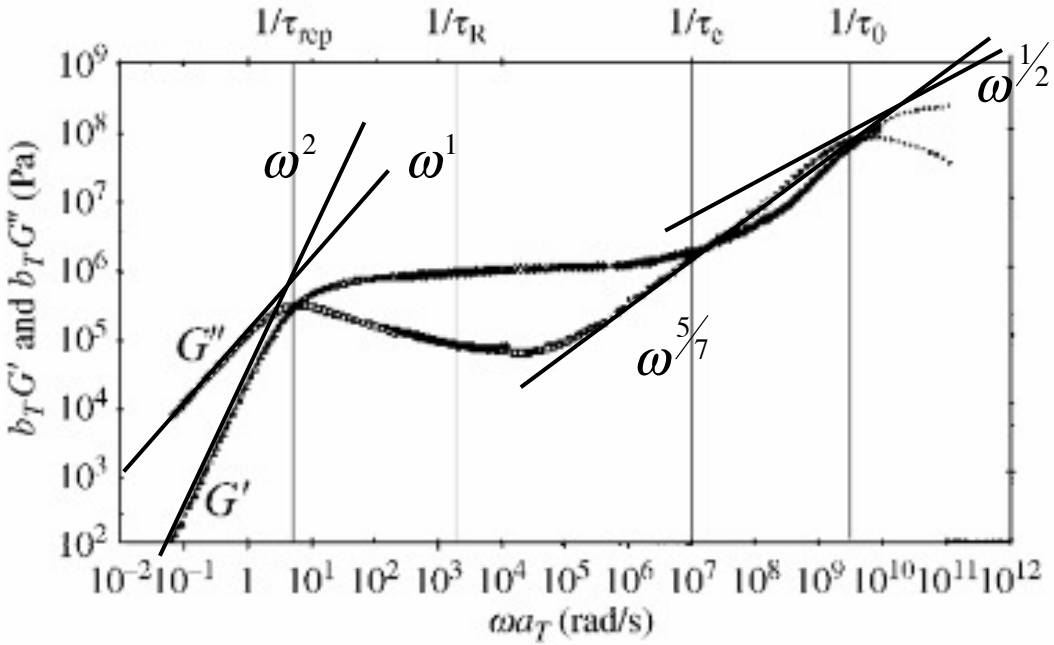

Fig. 9.3
Master curve at 25 °C from oscillatory shear data at six temperatures for a 1,4-polybutadiene sample with $M_w = 130\,000\ \mathrm{g\,mol^{-1}}$. Data from R. H. Colby, L. J. Fetters and W. W. Graessley, *Macromolecules* **20**, 2226 (1987).

Lodge Liquid and Transient Network Model

$$\boldsymbol{\sigma}(t) = -\int_{t'=-\infty}^{t} G(t-t')\frac{\mathrm{d}\mathbf{B}(t,t')}{\mathrm{d}t'}\,\mathrm{d}t'$$

$$\mathbf{B}(t,t') = \begin{pmatrix} 1+(\gamma(t)-\gamma(t'))^2 & 0 & \gamma(t)-\gamma(t') \\ 0 & 1 & 0 \\ \gamma(t)-\gamma(t') & 0 & 1 \end{pmatrix}$$

Simple Shear Finger Tensor

$$\sigma_{zx}(t) = \int_{t'=-\infty}^{t} G(t-t')\frac{\mathrm{d}\gamma}{\mathrm{d}t'}\,\mathrm{d}t'$$

Simple Shear Stress

$$(\sigma_{xx}-\sigma_{zz})(t) = 2\int_{t'=-\infty}^{t} G(t-t')(\gamma(t)-\gamma(t'))\frac{\mathrm{d}\gamma}{\mathrm{d}t'}\,\mathrm{d}t'$$

First Normal Stress

$$\sigma_{yy}-\sigma_{zz} = 0$$

Second Normal Stress

For a Hookean Elastic $G = \text{const}$

$$\sigma_{zx}(t) = G\gamma(t) \ ,$$

$$(\sigma_{xx} - \sigma_{zz})(t) = 2G \int_{t'=0}^{t} (\gamma(t) - \gamma(t')) \frac{\mathrm{d}\gamma}{\mathrm{d}t'} \, \mathrm{d}t'$$

$$= G\gamma^2(t) \ .$$

For Newtonian Fluid

$$G(t-t') = \eta\delta(t-t')$$

$$\sigma_{zx}(t) = \eta\frac{\mathrm{d}\gamma}{\mathrm{d}t}$$

$$(\sigma_{xx} - \sigma_{zz})(t) = 0\ ,$$

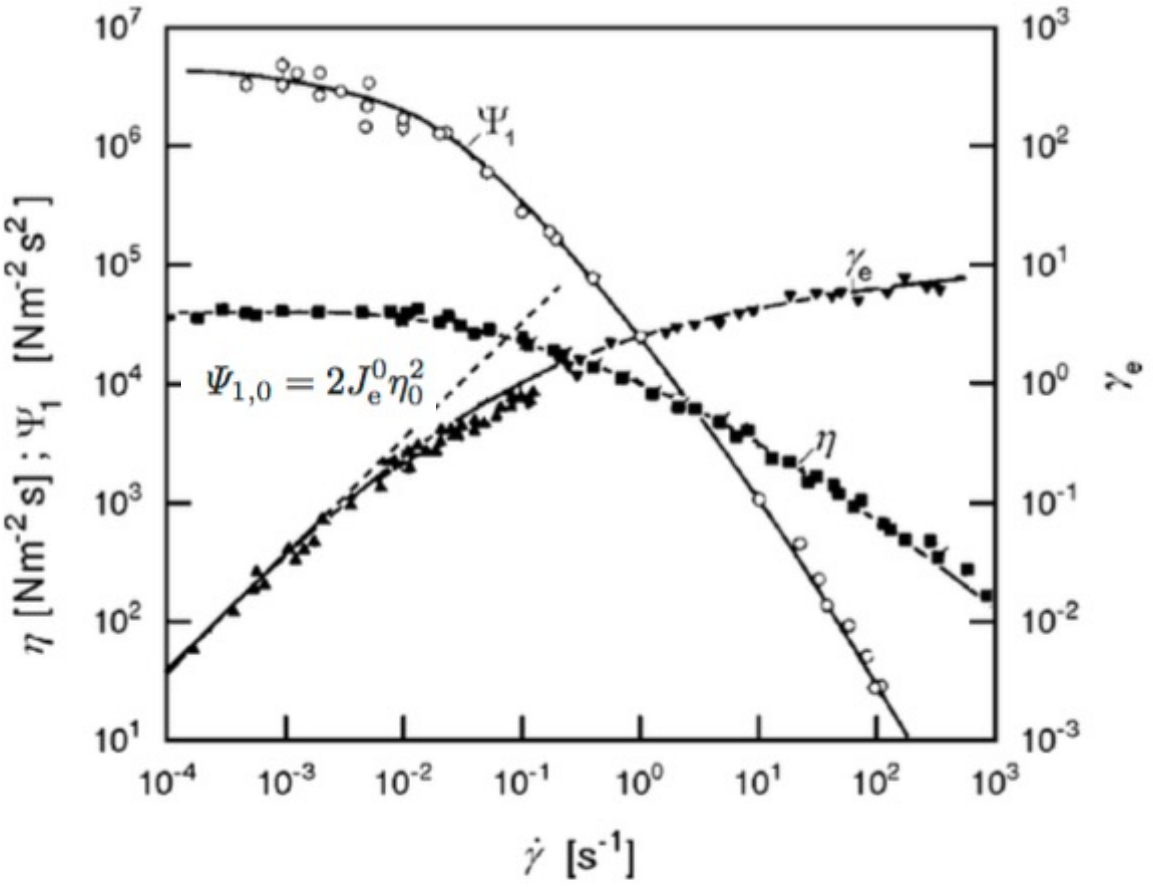

Fig. 9.17. PE under steady state shear flow at 150 °C: Strain rate dependencies of the viscosity η, the primary normal stress coefficient Ψ_1 and the recoverable shear strain γ_e. The *dotted line* represents Eq. (9.157). Results obtained by Laun [116]

Dumbbell Model

$$dx/dt = -(dU/dx)/z + g(t) = -kx/z + g(t)$$

$$x(t) = \int_{-\infty}^{t} dt' \exp\left(\frac{-k(t-t')}{\xi}\right) g(t)$$

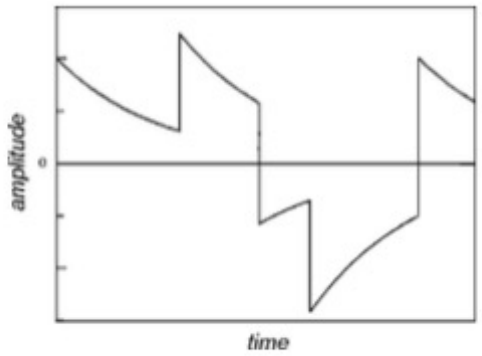

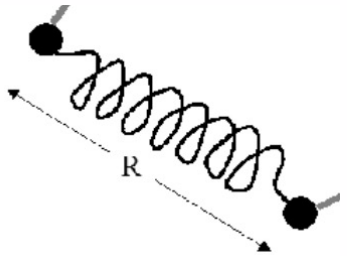

Fig. 8.4. Time dependence of the amplitude Z_m of a Rouse mode (schematic)

$$\langle x(t_1)x(0)\rangle = kT \exp(-t/t)/k$$

Dilute Solution Chain

Dynamics of the chain

Rouse Motion

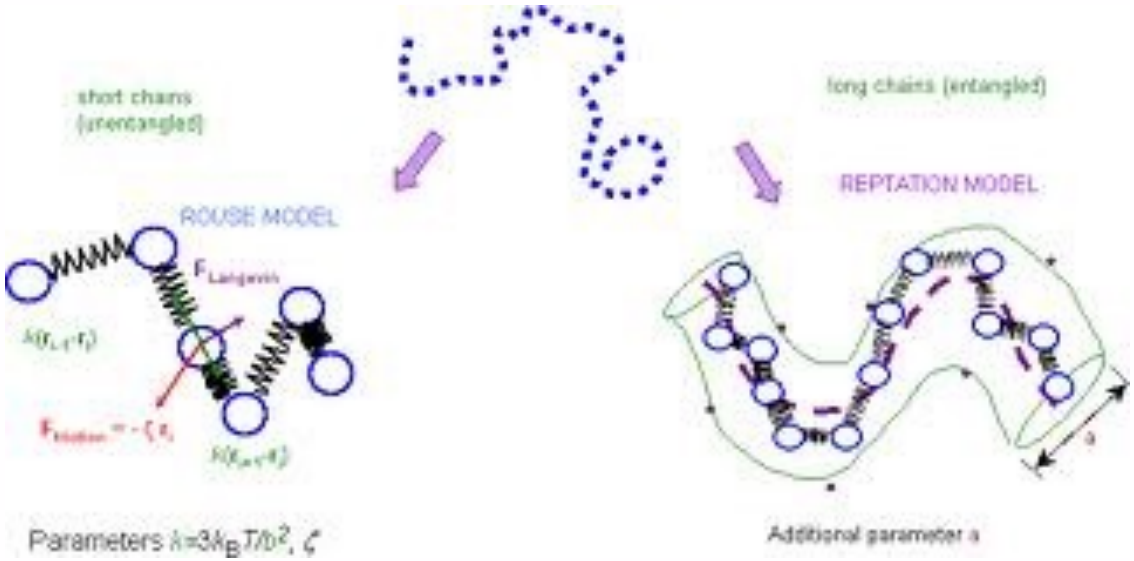

$$E = \frac{k_{spr}}{2}\sum_{i=1}^{N}\left(R_i - R_{i-1}\right)^2$$

$$\frac{dR_i}{dt} = \frac{-\left(dE/dR_i\right)}{\xi} + g_i(t)$$

$$\xi = 6\pi\eta_{solvent}a$$

Beads 0 and N are special

For Beads 1 to N-1

$$\frac{dR_i}{dt} = \frac{-k_{spr}}{\xi}\left(R_{i+1} + R_{i-1} - 2R_i\right) + g_i(t)$$

For Bead 0 use $R_{-1} = R_0$ and for bead N $R_{N+1} = R_N$

This is called a closure relationship

Dilute Solution Chain

Dynamics of the chain

Rouse Motion

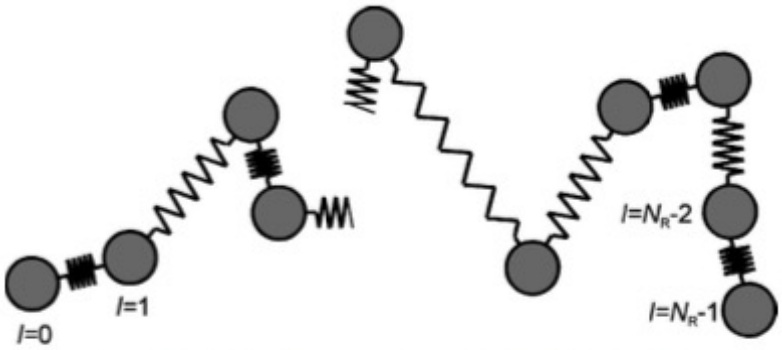

Fig. 8.1. Rouse chain composed of N_R beads connected by springs

$$\frac{dR_i}{dt} = \frac{-k_{spr}}{\xi}\left(R_{i+1} + R_{i-1} - 2R_i\right) + g_i(t)$$

$$\zeta_R \, d\mathbf{r}_l/dt = b_R \, (\mathbf{r}_{l+1} - \mathbf{r}_l) + b_R \, (\mathbf{r}_{l-1} - \mathbf{r}_l)$$
$$= b_R \, (\mathbf{r}_{l+1} + \mathbf{r}_{l-1} - 2\,\mathbf{r}_l)$$

The Rouse unit size is arbitrary so we can make it very small and:

$$\frac{dR}{dt} = \frac{-k_{spr}}{\xi}\frac{d^2R}{di^2} + g_i(t)$$

With dR/dt = 0 at i = 0 and N

$$\frac{d^2R}{di^2}$$

Reflects the curvature of R in i,
it describes modes of vibration like on a guitar string

x, y, z decouple (are equivalent) so you can just deal with z

$$\zeta_R \frac{dz_l}{dt} = b_R(z_{l+1} - z_l) + b_R(z_{l-1} - z_l)$$

$$\zeta_R \, d\mathbf{r}_l/dt = b_R \, (\mathbf{r}_{l+1} - \mathbf{r}_l) + b_R \, (\mathbf{r}_{l-1} - \mathbf{r}_l)$$
$$= b_R \, (\mathbf{r}_{l+1} + \mathbf{r}_{l-1} - 2\,\mathbf{r}_l)$$

For a chain of infinite molecular weight there are wave solutions to this series of differential equations

$$z_l \sim \exp\left(-\frac{t}{\tau}\right)\exp(il\delta)$$

Phase shift between adjacent beads

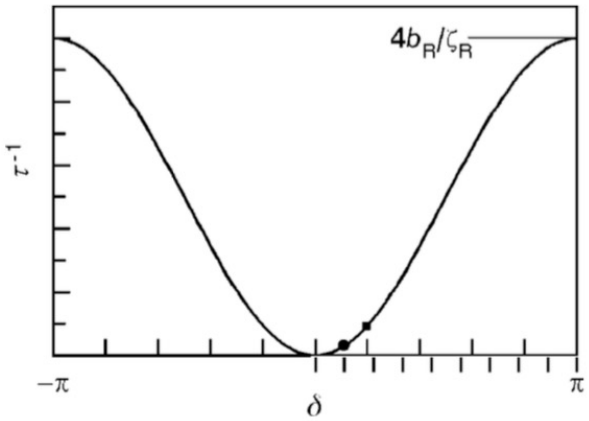

Fig. 8.2. Relaxation rates of Rouse modes as a function of the phase shift δ. *Marks on the inside* of the abscissa show the mode positions for a cyclic chain with $N_R = 10$ beads, the *marks on the outside* give the modes of a linear chain with the same length. The lowest order Rouse modes of the two chains with relaxation rates τ_R^{-1} are especially indicated by a *filled square* and a *filled circle*

Use the proposed solution in the differential equation results in:

$$\tau^{-1} = \frac{b_R}{\zeta_R}(2 - 2\cos\delta) = \frac{4b_R}{\zeta_R}\sin^2\frac{\delta}{2}$$

For N_R = 10

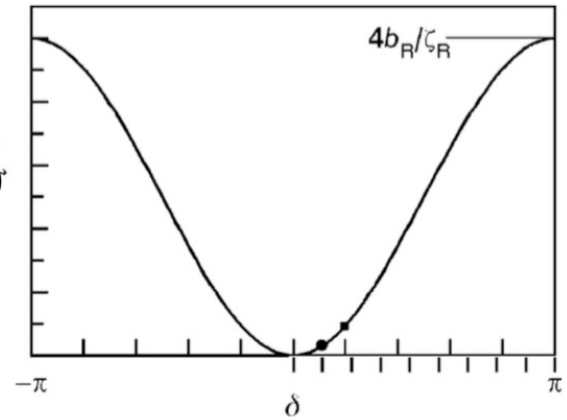

Fig. 8.2. Relaxation rates of Rouse modes as a function of the phase shift δ. *Marks on the inside* of the abscissa show the mode positions for a cyclic chain with $N_R = 10$ beads, the *marks on the outside* give the modes of a linear chain with the same length. The lowest order Rouse modes of the two chains with relaxation rates τ_R^{-1} are especially indicated by a *filled square* and a *filled circle*

$$\tau^{-1} = \frac{b_R}{\zeta_R}(2 - 2\cos\delta) = \frac{4b_R}{\zeta_R}\sin^2\frac{\delta}{2}$$

Cyclic Boundary Conditions:

$$z_l = z_{l+N_R}$$

$$N_R\delta = m2\pi$$

N_R values of phase shift

$$\delta_m = \frac{2\pi}{N_R}m; \quad m = -\left(\frac{N_R}{2} - 1\right),\ldots,\frac{N_R}{2}$$

For N_R = 10

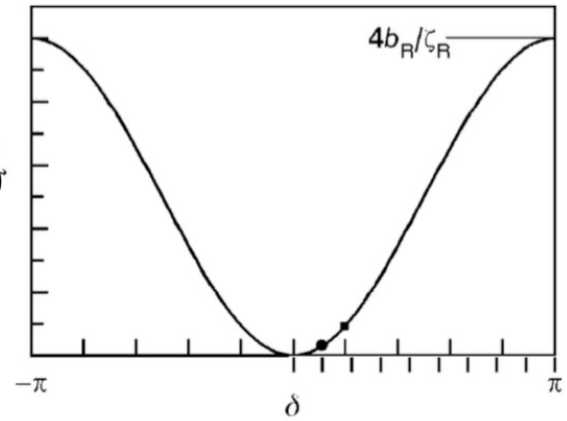

Fig. 8.2. Relaxation rates of Rouse modes as a function of the phase shift δ. *Marks on the inside* of the abscissa show the mode positions for a cyclic chain with $N_R = 10$ beads, the *marks on the outside* give the modes of a linear chain with the same length. The lowest order Rouse modes of the two chains with relaxation rates τ_R^{-1} are especially indicated by a *filled square* and a *filled circle*

$$\tau^{-1} = \frac{b_R}{\zeta_R}(2 - 2\cos\delta) = \frac{4b_R}{\zeta_R}\sin^2\frac{\delta}{2}$$

Free End Boundary Conditions:

$$z_l - z_0 = z_{N_R-1} - z_{N_R-2} = 0$$

$$\frac{dz}{dl}(l=0) = \frac{dz}{dl}(l = N_R - 1) = 0$$

$$(N_R - 1)\delta = m\pi$$

N_R values of phase shift

N_R Rouse Modes of order "m"

$$\delta_m = \frac{\pi}{(N_R - 1)}m; \quad m = 0,1,2,\ldots,(N_R - 1)$$

Lowest order relaxation time dominates the response

$$\tau_R = \frac{1}{3\pi^2} \frac{\left(\frac{\zeta_R}{a_R^2}\right)}{kT} R_0^4$$

This assumes that $\left(\frac{\zeta_R}{a_R^2}\right)$

is constant, friction coefficient is proportional to number of monomer units in a Rouse segment

This is the basic assumption of the Rouse model,

$$\zeta_R \sim a_R^2 \sim \frac{N}{N_R} = n_R$$

Lowest order relaxation time dominates the response

$$\tau_R = \frac{1}{3\pi^2} \frac{\left(\frac{\zeta_R}{a_R^2}\right)}{kT} R_0^4$$

Since $R_0^2 = a_0^2 N$

$$\tau_R \sim \frac{N^2}{kT}$$

The amplitude of the Rouse modes is given by:

$$\left\langle Z_m^2 \right\rangle = \frac{2}{3\pi^2} \frac{R_0^2}{m^2}$$

The amplitude is independent of temperature because the free energy of a mode is proportional to kT and the modes are distributed by Boltzmann statistics

$$p\left(Z_m\right) = \exp\left(-\frac{\left\langle F \right\rangle}{kT} \right)$$

90% of the total mean-square end to end distance of the chain originates from the lowest order Rouse-modes so the chain can be often represented as an elastic dumbbell

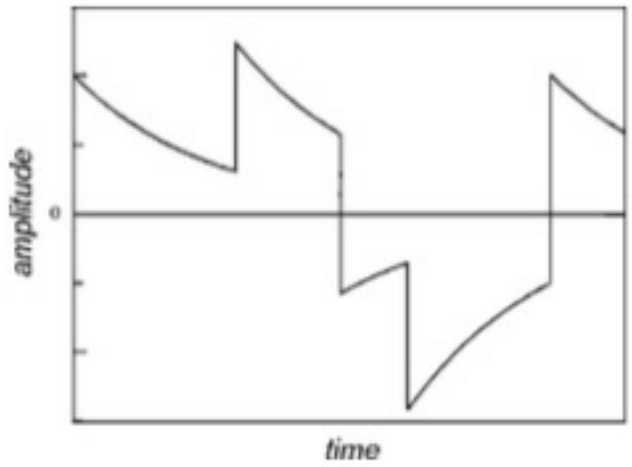

Fig. 8.4. Time dependence of the amplitude Z_m of a Rouse mode (schematic)

Rouse dynamics (like a dumbell response)

Dumbbell

$$\frac{dx}{dt} = -\frac{\left(\frac{dU}{dx}\right)}{\zeta} + g(t) = -\frac{k_{spr}x}{\zeta} + g(t)$$

$$x(t) = \int_{-\infty}^{t} dt' \exp\left(-\frac{t-t'}{\tau}\right) g(t)$$

$$\tau = \frac{\zeta}{k_{spr}}$$

Rouse

$$\tau_R = \frac{\zeta_R}{4b_R \sin^2 \frac{\delta}{2}}$$

$$\delta = \frac{\pi}{N_R - 1} m \ , \quad \text{m=0,1,2,...,}N_R\text{-1}$$

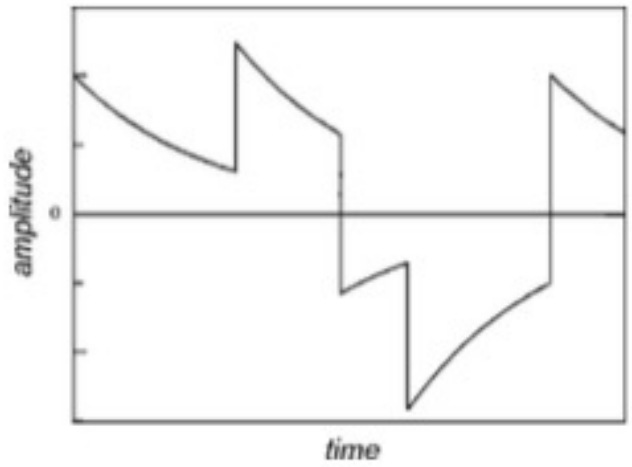

Fig. 8.4. Time dependence of the amplitude Z_m of a Rouse mode (schematic)

Rouse dynamics (like a dumbell response)

$\langle g(t_1)g(t_2)\rangle = 2D\delta(t)$ where $t = t_1 - t_2$ and $\delta(\ )$ is the delta function whose integral is 1

Also, $D = \dfrac{kT}{\zeta}$

$$\langle x(t)x(0)\rangle = \frac{kT\exp\left(-\dfrac{t}{\tau}\right)}{k_{spr}} \qquad \tau = \frac{\zeta}{k_{spr}}$$

For t => 0, $\langle x^2\rangle = \dfrac{kT}{k_{spr}}$

Predictions of Rouse Model

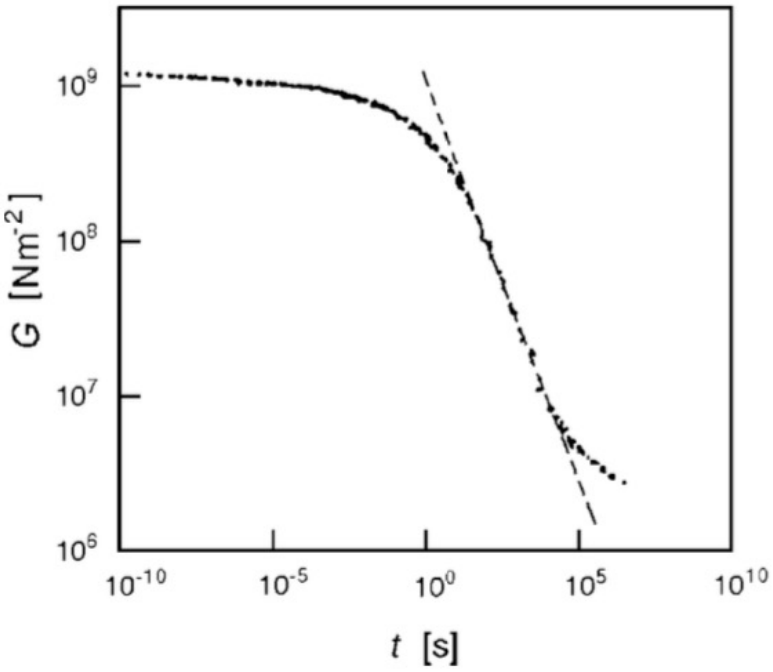

Fig. 8.6. Time-dependent shear modulus of PVC. Master curve set up for T_g = 65 °C as the reference temperature. The *dashed line* indicates the slope predicted by the Rouse model. Data from Eisele [101]

$$G(t) \sim t^{-\frac{1}{2}}$$

$$G'(\omega) \sim (\omega\eta_0)^{\frac{1}{2}}$$

$$\eta_0 = kT\rho_p\tau_R\frac{\pi^2}{12} \sim N$$

Newtonian Flow

Entanglement Reptation

Rouse Behavior

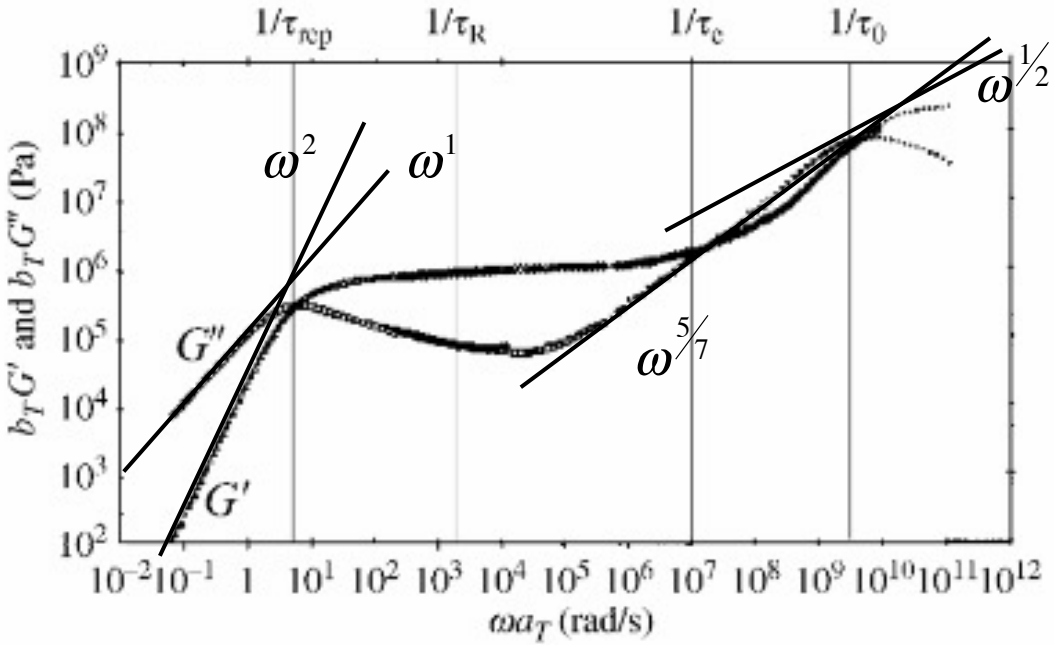

Fig. 9.3
Master curve at 25 °C from oscillatory shear data at six temperatures for a 1,4-polybutadiene sample with $M_w = 130\,000\ \mathrm{g\,mol^{-1}}$. Data from R. H. Colby, L. J. Fetters and W. W. Graessley, *Macromolecules* **20**, 2226 (1987).

Dilute Solution Chain

Dynamics of the chain

Rouse Motion

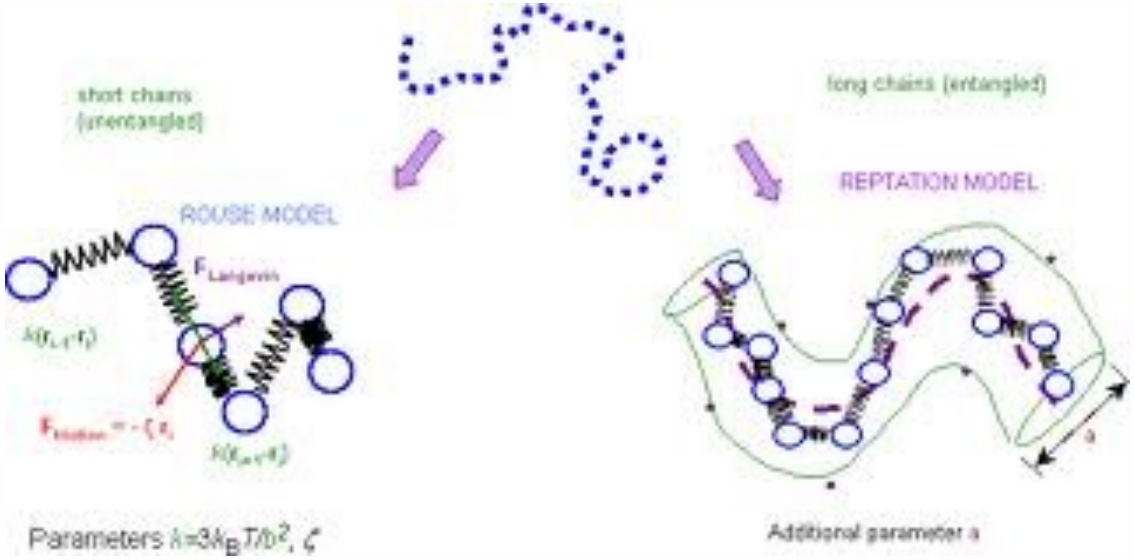

Predicts that the viscosity will follow N which is true for low molecular weights in the melt and for fully draining polymers in solution

Rouse model predicts
Relaxation time follows N^2 (actually follows N^3/df)
Diffusion constant follows 1/N (zeroth order mode is translation of the molecule) (actually follows $N^{-1/df}$)
Both failings are due to hydrodynamic interactions (incomplete draining of coil)

Dilute Solution Chain

Dynamics of the chain

Rouse Motion

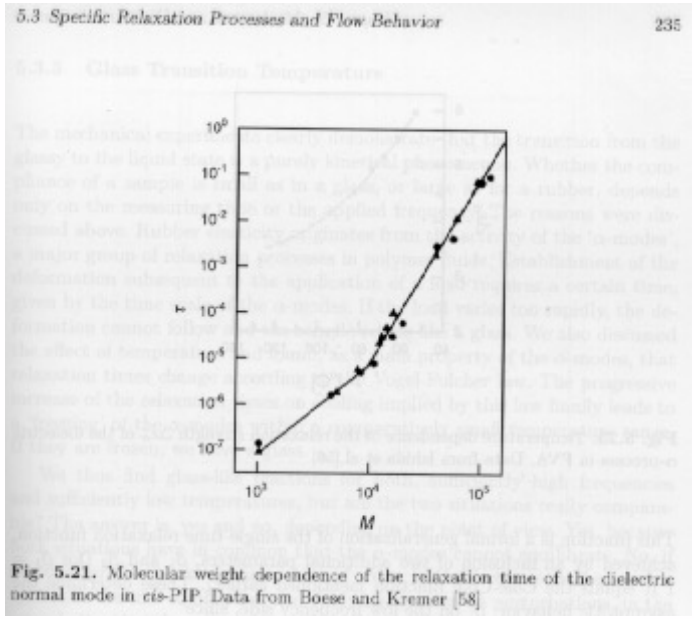

Fig. 5.21. Molecular weight dependence of the relaxation time of the dielectric normal mode in *cis*-PIP. Data from Boese and Kremer [58]

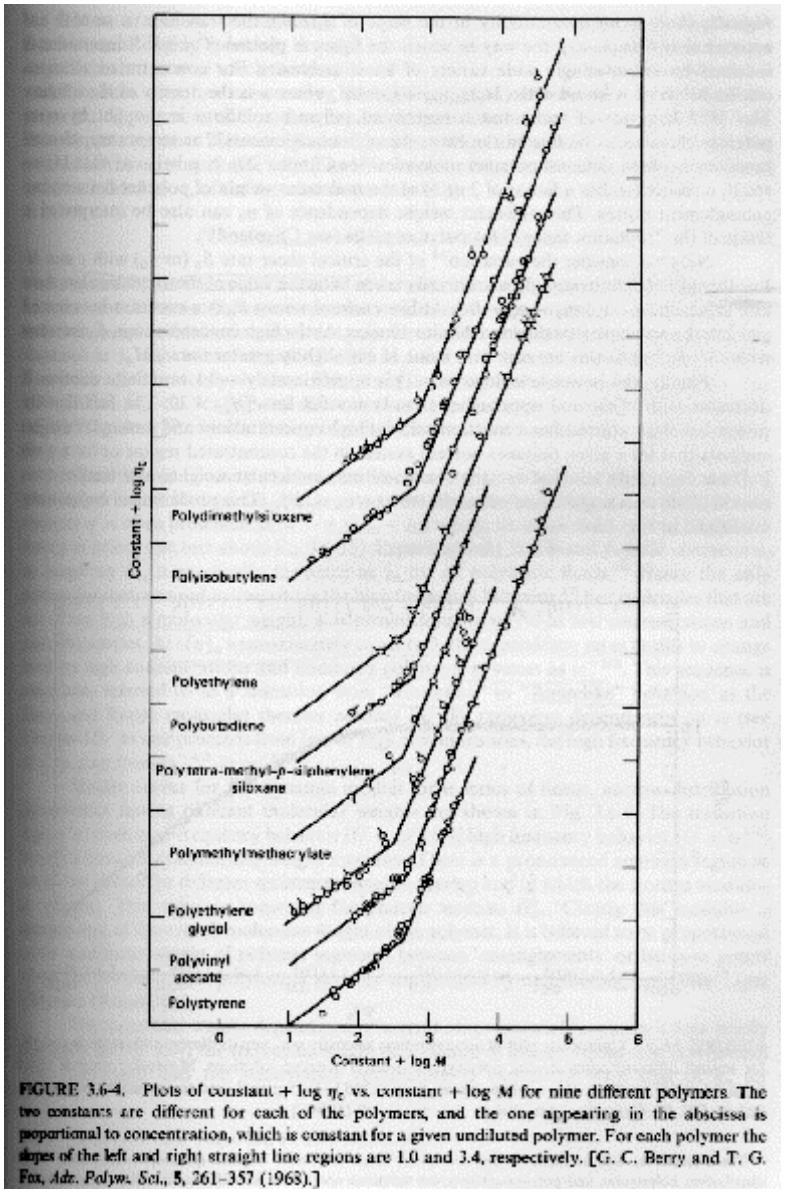

FIGURE 3.6-4. Plots of constant + log η_c vs. constant + log M for nine different polymers. The two constants are different for each of the polymers, and the one appearing in the abscissa is proportional to concentration, which is constant for a given undiluted polymer. For each polymer the slopes of the left and right straight line regions are 1.0 and 3.4, respectively. [G. C. Berry and T. G. Fox, *Adv. Polym. Sci.*, **5**, 261–357 (1968).]

Predicts that the viscosity will follow N which is true for low molecular weights in the melt and for fully draining polymers in solution

Rouse model predicts

Relaxation time follows N^2 (actually follows N^3/df)

Hierarchy of Entangled Melts

Chain dynamics in the melt can be described by a small set of "physically motivated, material-specific paramters"

Tube Diameter d_T
Kuhn Length l_K
Packing Length p

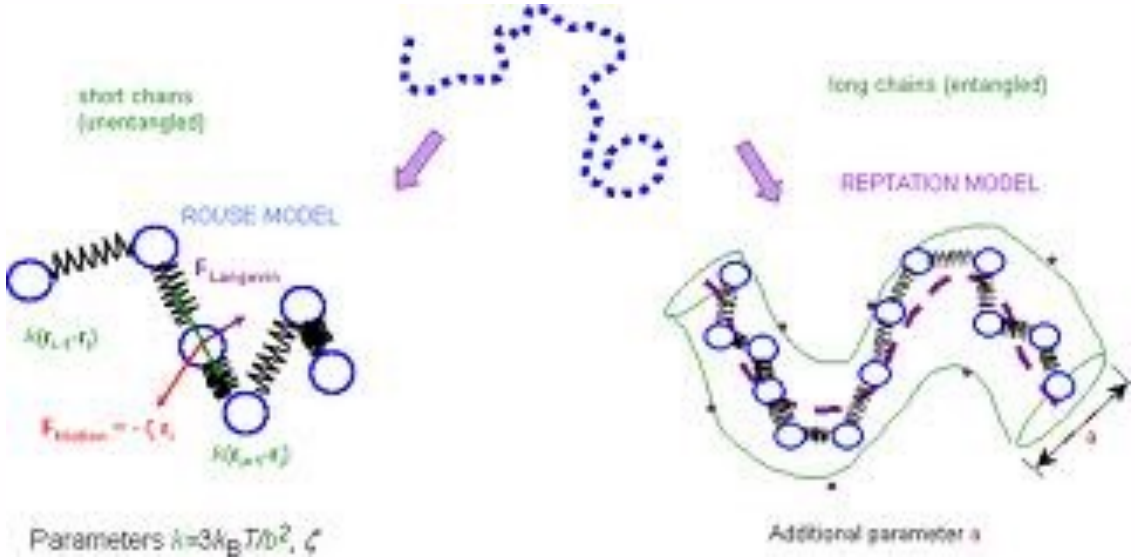

http://www.eng.uc.edu/~gbeaucag/Classes/MorphologyofComplexMaterials/SukumaranScience.pdf

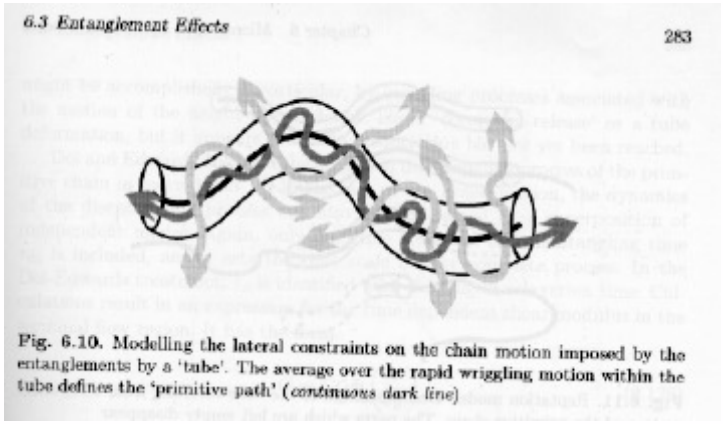

Fig. 6.10. Modelling the lateral constraints on the chain motion imposed by the entanglements by a 'tube'. The average over the rapid wriggling motion within the tube defines the 'primitive path' (*continuous dark line*)

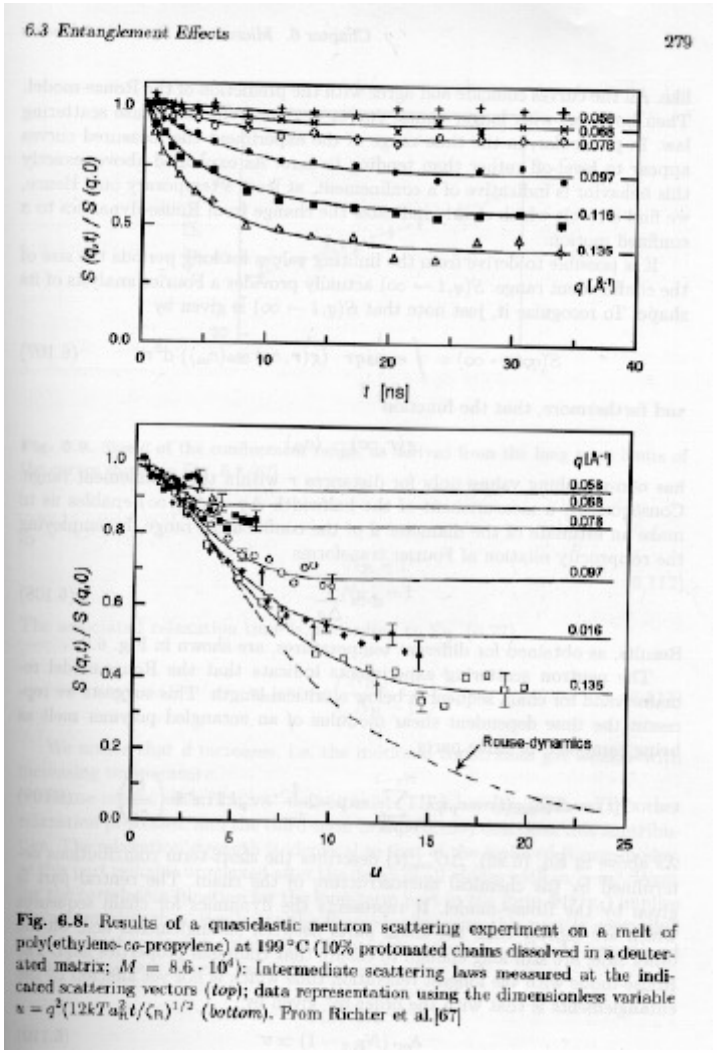

Fig. 6.8. Results of a quasielastic neutron scattering experiment on a melt of poly(ethylene-*co*-propylene) at 199 °C (10% protonated chains dissolved in a deuterated matrix; $M = 8.6 \cdot 10^4$): Intermediate scattering laws measured at the indicated scattering vectors (*top*); data representation using the dimensionless variable $u = q^2(12kTa_R^2t/\zeta_n)^{1/2}$ (*bottom*). From Richter et al.[67]

Quasi-elastic neutron scattering data
demonstrating the existence of the tube

Unconstrained motion => S(q) goes to 0 at very long times

Each curve is for a different q = 1/size

At small size there are less constraints (within the tube)

At large sizes there is substantial constraint (the tube)

By extrapolation to high times
a size for the tube can be obtained
d_T

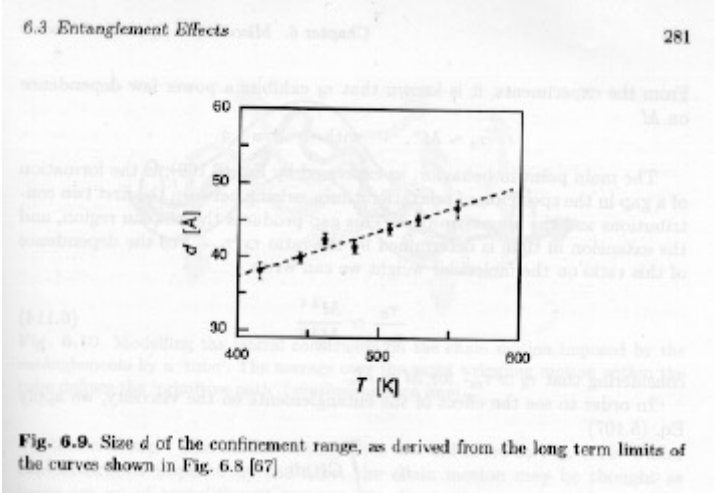

Fig. 6.9. Size d of the confinement range, as derived from the long term limits of the curves shown in Fig. 6.8 [67]

There are two regimes of hierarchy in time dependence
Small-scale unconstrained Rouse behavior
Large-scale tube behavior

We say that the tube follows a "primitive path"
This path can "relax" in time = Tube relaxation or Tube Renewal

Without tube renewal the Reptation model predicts that viscosity follows N^3 (observed is $N^{3.4}$)

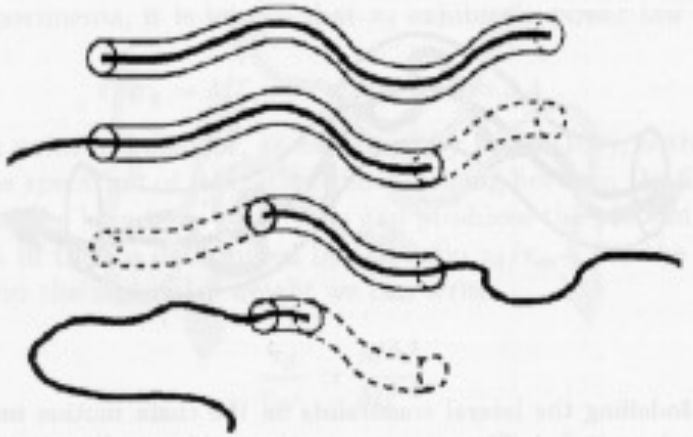

Fig. 6.11. Reptation model: Decomposition of the tube resulting from a reptative motion of the primitive chain. The parts which are left empty disappear

Without tube renewal the Reptation model predicts that viscosity follows N^3 (observed is $N^{3.4}$)

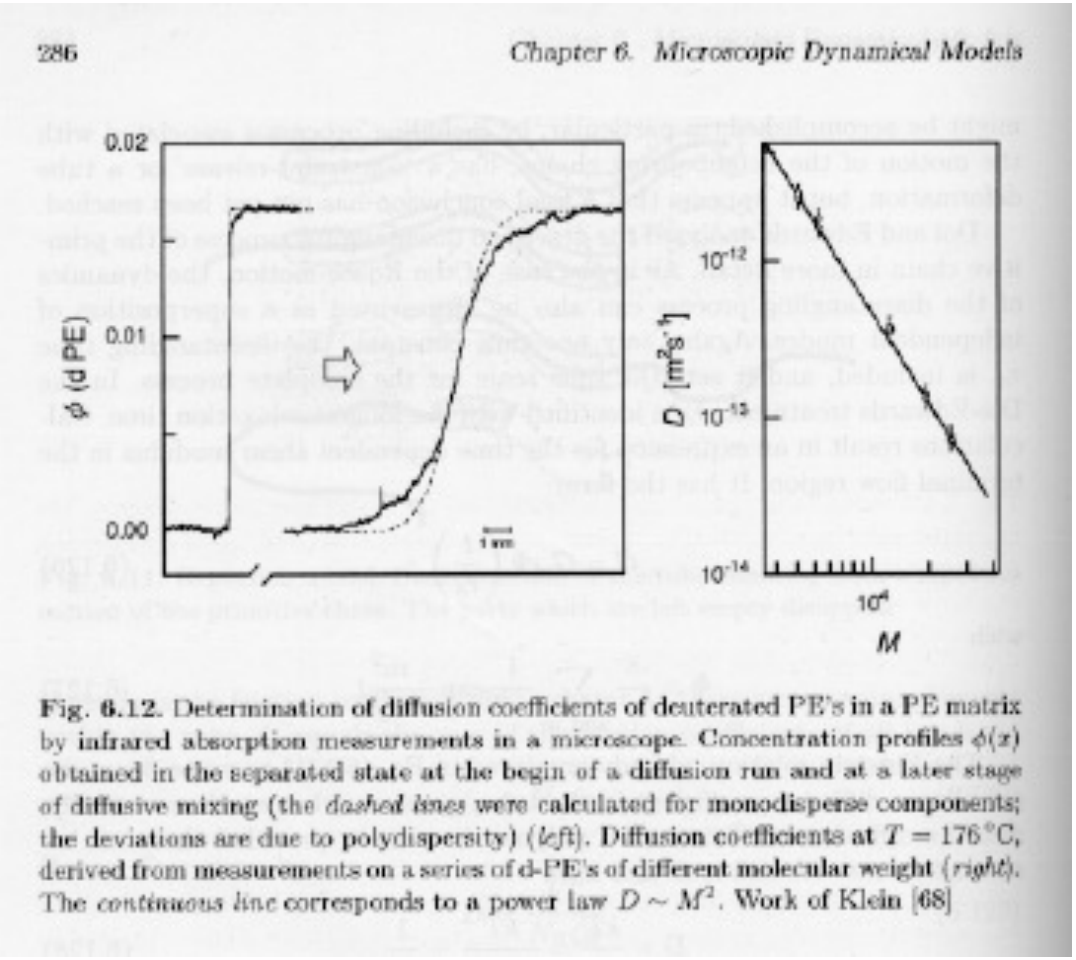

Fig. 6.12. Determination of diffusion coefficients of deuterated PE's in a PE matrix by infrared absorption measurements in a microscope. Concentration profiles $\phi(x)$ obtained in the separated state at the begin of a diffusion run and at a later stage of diffusive mixing (the *dashed lines* were calculated for monodisperse components; the deviations are due to polydispersity) (*left*). Diffusion coefficients at $T = 176\,^{\circ}\mathrm{C}$, derived from measurements on a series of d-PE's of different molecular weight (*right*). The *continuous line* corresponds to a power law $D \sim M^{-2}$. Work of Klein [68]

Reptation predicts that the diffusion coefficient will follow N^2 (Experimentally it follows N^2)
Reptation has some experimental verification
Where it is not verified we understand that tube renewal is the main issue.

(Rouse Model predicts D ~ 1/N)

Reptation of DNA in a concentrated solution

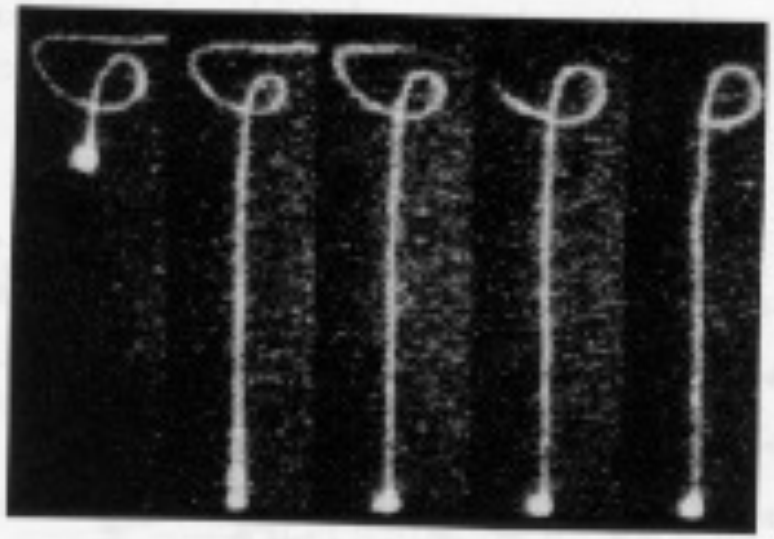

Fig. 6.13. Series of images of a fluorescently stained DNA chain embedded in a concentrated solution of unstained chains: Initial conformation (*left*); partial stretching by a rapid move of the bead at one end (*second from the left*); chain recoil by a reptative motion in the tube (*subsequent pictures to the right*). Reprinted with permission from T.Perkins, D.E.Smith and S.Chu. *Science*, 264:819, 1994. Copyright (1994) American Association for the Advancement of Science

Simulation of the tube

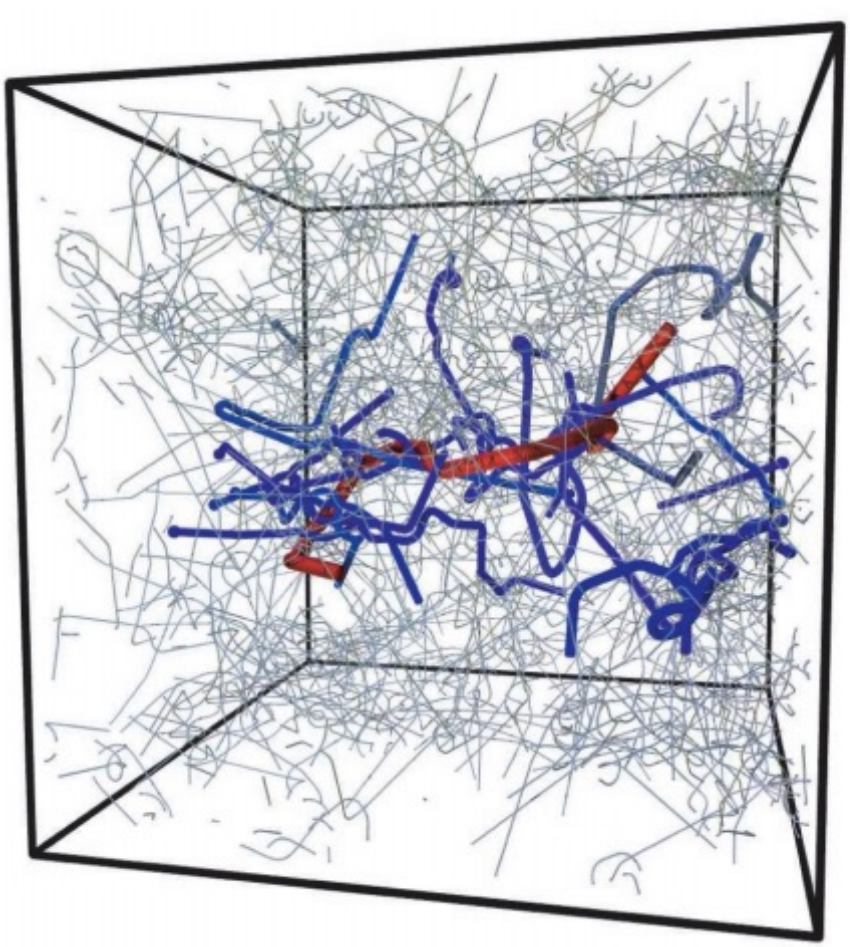

Fig. 3. Result of the primitive-path analysis of a melt of 200 chains of $N + 1 = 350$ beads. We show the primitive path of one chain (red) together with all of those it is entangled with (blue). The primitive paths of all other chains in the system are shown as thin lines.

Simulation of the tube

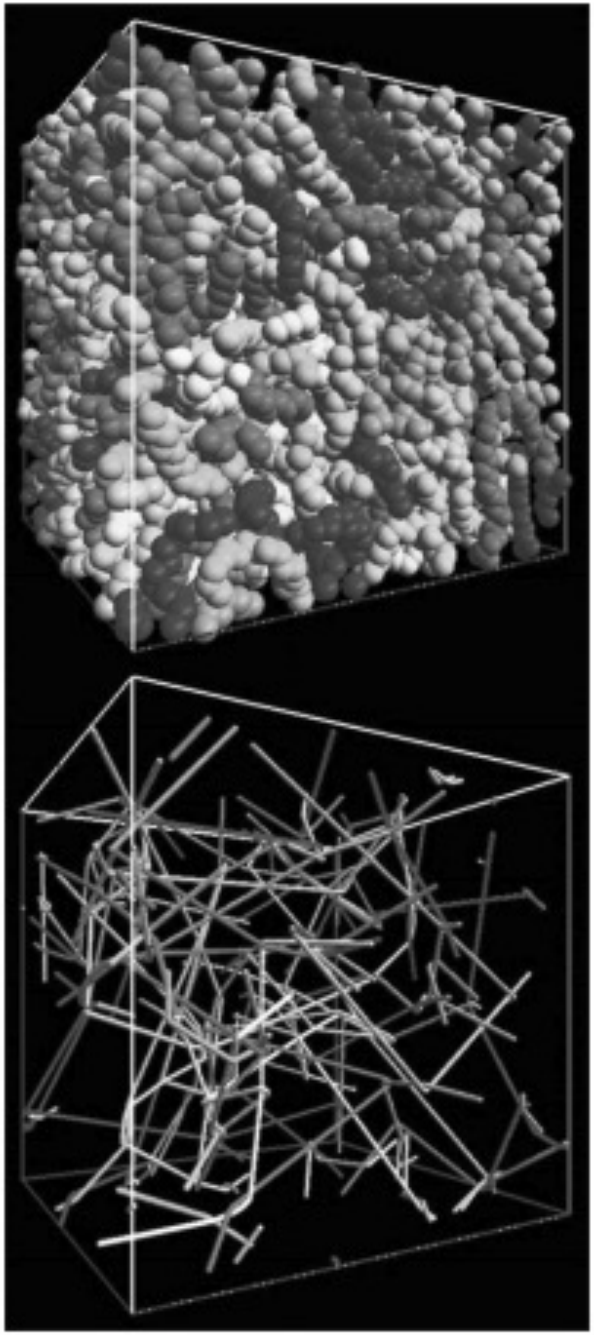

Fig. 3. A representative amorphous polymer sample and the corresponding network of primitive paths.

Plateau Modulus

Not Dependent on N, Depends on T and concentration

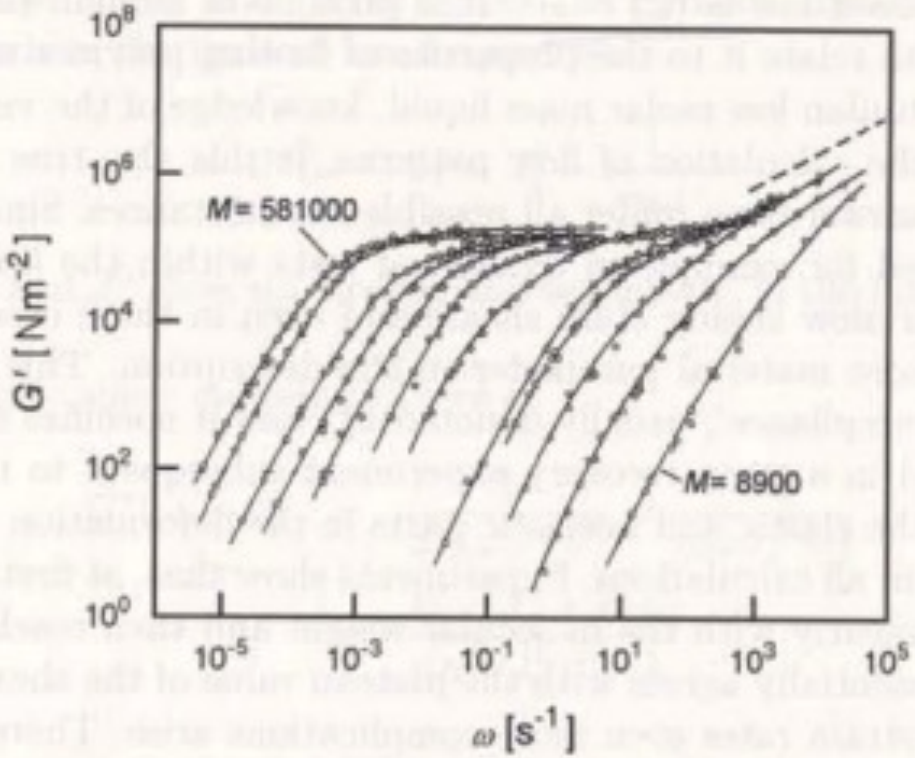

Fig. 5.15. Storage shear moduli measured for a series of fractions of PS with different molecular weights in the range $M = 8.9 \cdot 10^3$ to $M = 5.81 \cdot 10^5$. The *dashed line* in the upper right corner indicates the slope corresponding to the power law Eq. (6.81) derived for the Rouse-model of the glass-transition. Data from Onogi et al.[54]

$$G_0 = \frac{4\rho RT}{5M_e} = \frac{4RT}{5p^3}$$

Kuhn Length- conformations of chains $\langle R^2 \rangle = l_K L$

Packing Length- length were polymers interpenetrate $p = 1/(\rho_{chain} \langle R^2 \rangle)$
where ρ_{chain} is the number density of monomers

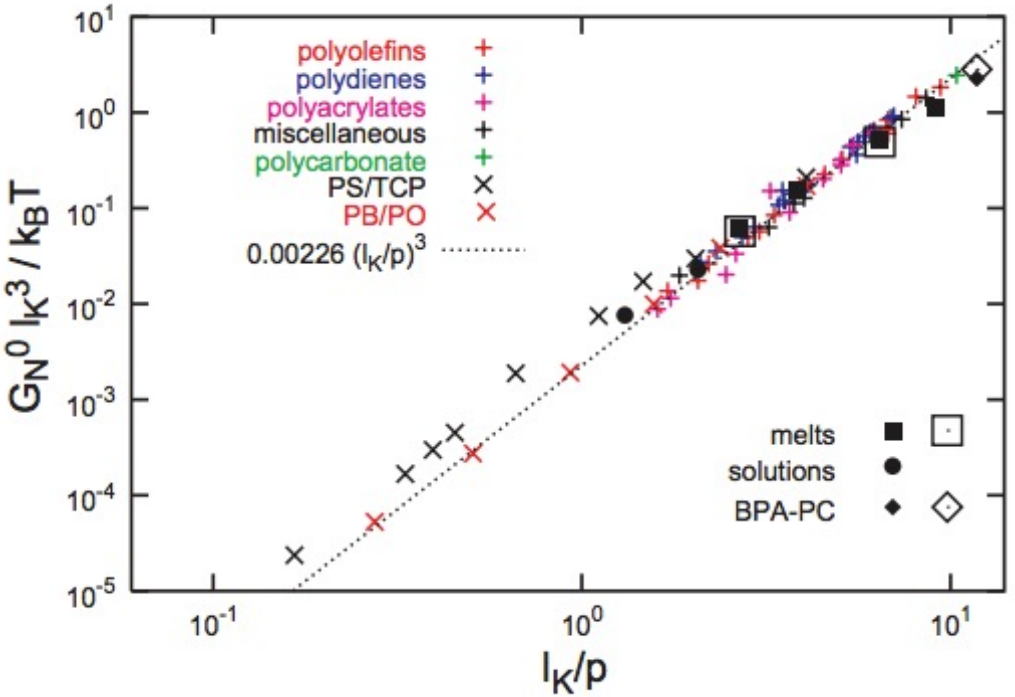

Fig. 2. Dimensionless plateau moduli Gl_K^3/k_BT as a function of the dimensionless ratio l_K/p of Kuhn length l_K and packing length p. The figure contains (i) experimentally measured plateau moduli for polymer melts (*25*) (+; colors mark different groups of polymers as indicated) and semidilute solutions (*26–28*) (×); (ii) plateau moduli inferred from the normal tensions measured in computer simulation of bead-spring melts (*35, 36*) (□) and a semi-atomistic polycarbonate melt (*37*) (◇) under an elongational strain; and (iii) predictions of the tube model Eq. 1 based on the results of our primitive-path analysis for bead-spring melts (■), bead-spring semidilute solutions (●), and the semi-atomistic polycarbonate melt (◆). The line indicates the best fit to the experimental data for polymer melts by Fetters *et al.* (*24*). Errors for all the simulation data are smaller than the symbol size.

this implies that $d_T \sim p$

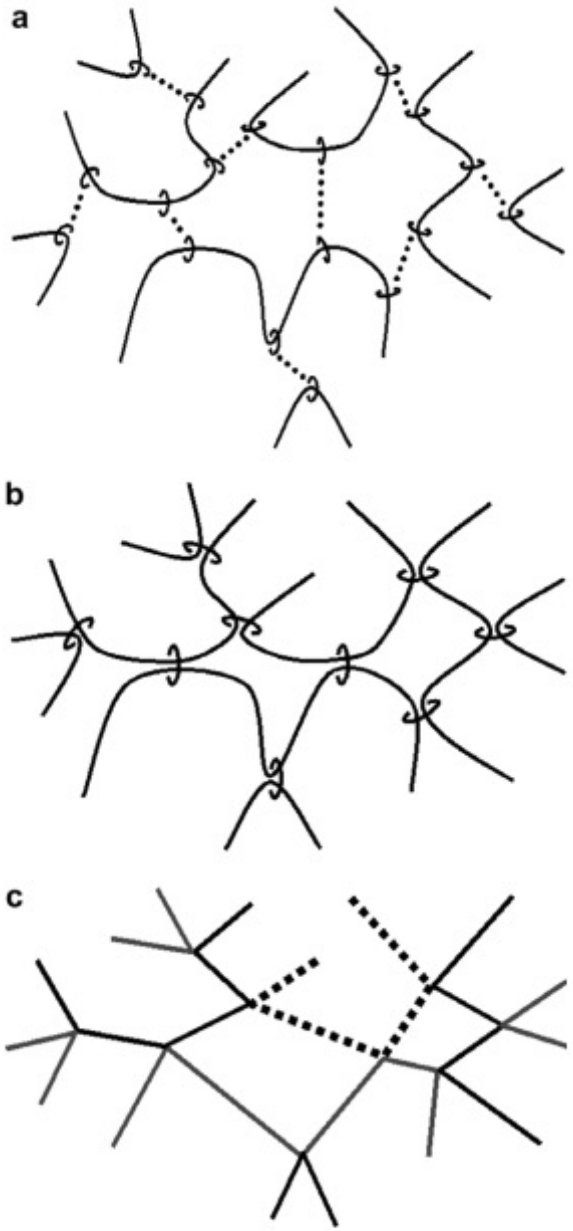

Fig. 1. Schematic representation of dual slip-links. (a) Chains coupled by virtual links. (b) Dual slip-links. (c) Real space representation of the corresponding network of primitive paths.

McLeish/Milner/Read/Larsen Hierarchical Relaxation Model

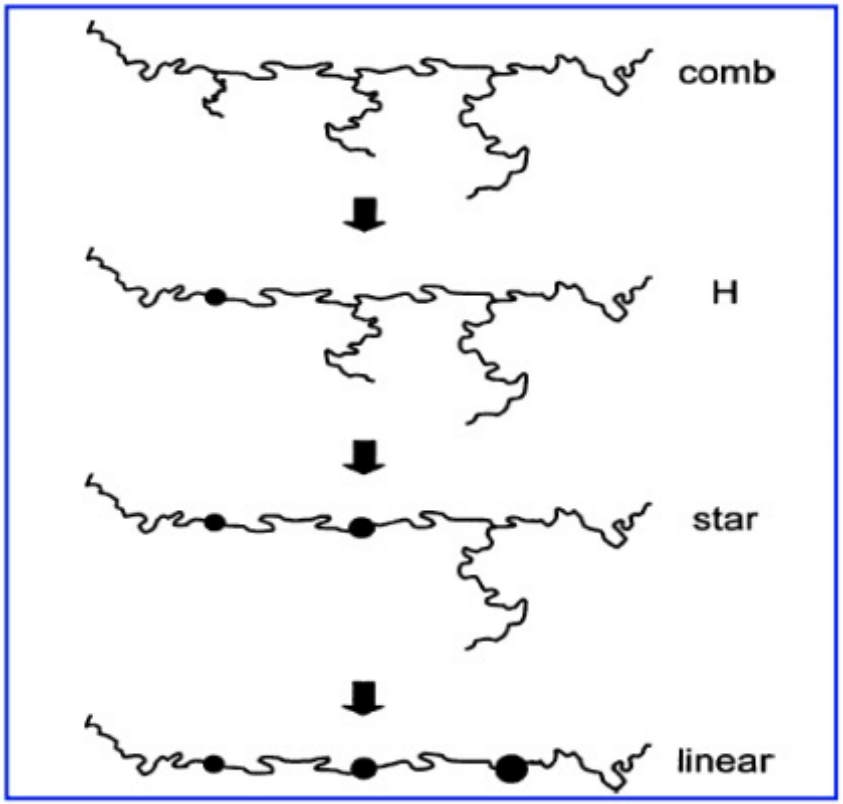

http://www.engin.umich.edu/dept/che/research/larson/downloads/Hierarchical-3.0-manual.pdf